

# Team Results Document

SenseNC



SenseNC

## University: NC State University

### Team members:

Ashley Dehn  
Charlie Capitano  
Lauren Mabe  
Jenny Lopez  
Ameerah Abazid  
Lily Ro  
Ben Cole  
Jayden Ford

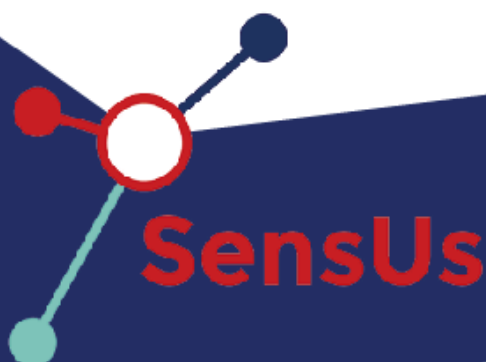
### Supervisors:

Dr. Michael Daniele  
Dr. Stefano Menegatti

### Coaches:

Lina Acosta-Pérez  
M. Irfan Ismail

08/08/2025



SensUs 2025  
Acute Kidney Injury

## 1. Abstract

Acute Kidney Injury (AKI) affects over 13 million people annually and is a major contributor to postoperative morbidity and mortality. Current creatinine monitoring relies on intermittent blood sampling and laboratory analysis, often delaying diagnosis or discharge. Here, we present a wearable electrochemical biosensor for real-time, continuous monitoring of creatinine in interstitial fluid (ISF), with a sensitivity of 27 nA/ $\mu$ M and a dynamic range of 0-230  $\mu$ M. The biosensor utilizes a copper-tetrakis(4-carboxyphenyl)porphyrin metal-organic framework (Cu-TCPP MOF) as the selective and reversible biorecognition element, exploiting copper's coordination chemistry with creatinine. A functionalized microneedle embedded with laser-induced graphene (LIG) electrodes transduces redox events via cyclic voltammetry (CV), yielding a reproducible oxidation peak at 84 mV, with oxidation current proportional to creatinine concentration. A custom wearable potentiostat acquires creatinine levels every 15 minutes over a 10-day period and wirelessly transmits data via Bluetooth™. A proprietary algorithm analyzes CV profiles to estimate creatinine concentration and glomerular filtration rate (GFR) in real time, with outputs accessible to both patients and clinicians. This low-cost, non-invasive platform offers a scalable solution for continuous kidney function assessment, reducing reliance on centralized laboratory testing and enabling earlier intervention or expedited discharge from the hospital.

## 2. AP Award: Biosensor Developed for the Eindhoven Testing Event

### 2.1. Molecular Recognition: Copper Metal-Organic Frameworks

In our previous design, copper served as the biorecognition element due to its well-established affinity for creatinine via metal-ligand coordination. Cyclic voltammetry (CV) in deionized (DI) water revealed two distinct oxidative peaks, confirming Cu-creatinine complex formation. The first peak, at lower potential, was attributed to free  $\text{Cu}^{2+}$  oxidation; the second, at higher potential, corresponded to oxidation of  $\text{Cu}^{2+}$  coordinated with creatinine, indicating spontaneous complexation (Section 8.1). These results demonstrate the feasibility of copper-based electrochemical sensing for selective creatinine detection and laid the foundation for development of continuous, reversible monitoring in interstitial skin fluid (ISF).

**This year, we advanced the biosensor's specificity and stability by engineering a non-biological recognition element using a copper-based metal-organic framework.** Specifically, we employed a Cu-TCPP, a Cu-MOF composed of copper(II) ions and tetrakis(4-carboxyphenyl)porphyrin (TCPP) ligands, as the biorecognition material (Xu et al., 2012). This framework enhances the accessibility and coordination environment of copper centers, enabling more consistent and selective creatinine binding under physiological conditions. The MOF is synthesized via a solvothermal reaction of  $\text{Cu}(\text{NO}_3)_2$ ,  $\text{H}_2\text{TCPP}$ , and a solvent mixture, as described in Section 8.2. The resulting MOF is ultrasonicated with Nafion<sup>TM</sup> and MilliQ water to create a colloidal suspension, which is drop-cast onto the working electrode (WE). Nafion<sup>TM</sup> improves adhesion and conductivity between the sensing element and electrode. Its negatively charged sulfate groups and hydrated pore network exclude negatively charged and larger species (e.g., proteins) while allowing small, positively charged molecules like creatinine to pass (Tsai et al., 2023).

As shown in Fig. 1a, our three-electrode system consists of an Ag/AgCl reference electrode (RE), a graphene counter electrode (CE), and a WE functionalized with Cu-TCPP. The Ag/AgCl RE provides a stable, well-characterized potential in aqueous environments, while the graphene CE offers high conductivity, chemical inertness, and a large surface, making it ideal for biosensing applications. This configuration supports reproducible measurements in ISF and is compatible with miniaturized, wearable formats (Grieshaber et al., 2008). Based on prior results and literature, creatinine undergoes enol tautomerization upon interaction with  $\text{Cu}^{2+}$  ions in ISF, increasing its partial positive charge and facilitating coordination through its cyclic amine nitrogen (Gao et al., 2013).

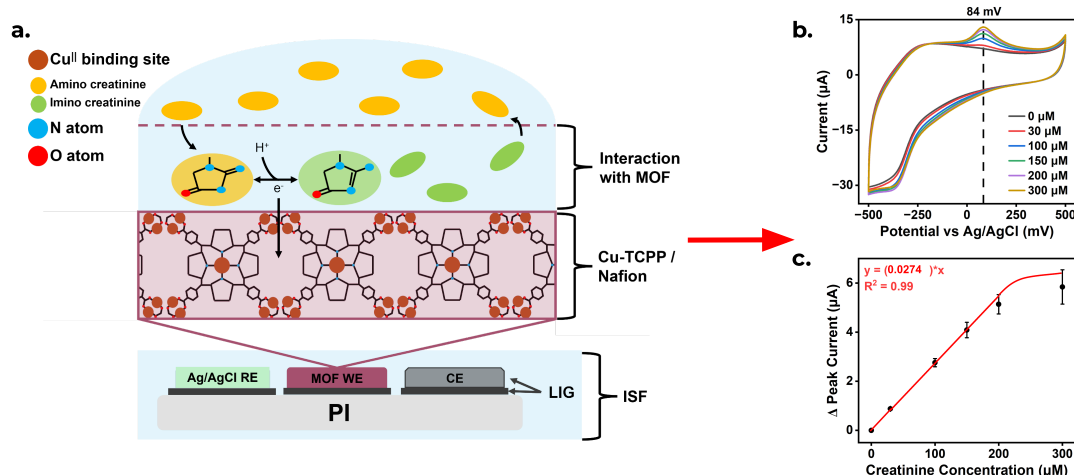


**Fig. 1.** Detection of creatinine in our ETE biosensor. Sensing begins at (a) the WE surface; as creatinine molecules interact with the WE surface, the presence of copper ions catalyzes their tautomerization through an oxidation reaction that is (b) detectable via CV. An oxidative peak occurred consistently at 84 mV, enabling the creation of (c) a calibration curve relating current to creatinine concentration.

While free  $\text{Cu}^{2+}$  readily forms stable complexes with tautomerized creatinine, steric constraints at coordination sites within the Cu-TCPP MOF reduce binding affinity. This steric modulation prevents irreversible complexation, promoting rapid dissociation (fast off-rates) as the local creatinine level drops. Consequently, the MOF surface dynamically

regenerates active  $\text{Cu}^{2+}$  sites, allowing reversible interactions and continuous sensing of both rising and falling creatinine concentrations. This transient binding mechanism is essential for real-time monitoring, as it maintains equilibrium with ambient ISF and prevents signal saturation.

## 2.2. Physical Transduction: Custom Laser-Induced Graphene Electrodes

The transduction electrodes are fabricated from laser-induced graphene (LIG), which offers high conductivity, electrochemical stability, and a porous 3D surface ideal for sensing. As detailed in Section 8.3, LIG is produced by laser-scribing commercial polyimide (PI) films with a carbon dioxide ( $\text{CO}_2$ ) laser under ambient conditions. This direct-write method thermally decomposes the polymer, converting the surface into a hierarchical graphene structure without additional processing or annealing. The resulting electrodes provide excellent flexibility, scalability, and a robust interface for Cu-TCPP MOF functionalization (Chen et al., 2022; Johnson et al., 2021; Ye et al., 2018). This enables three custom-patterned electrodes with high electroactive surface area in the sensing region. Cu-TCPP suspension is drop-cast onto the WE, Ag/AgCl is plated on the RE, and the CE remains bare graphene.

Enol tautomerization occurs when creatinine adheres to the sensor surface, transferring a proton from the solution and increasing its charge. This transition yields a consistent oxidation peak at 84 mV during CV, generating a calibration curve for creatinine concentrations from 0–300  $\mu\text{M}$  (Fig. 1c). Utilizing this calibration curve, the sensitivity was determined to be 27 nA/ $\mu\text{M}$  and the dynamic range was determined to be 0–230  $\mu\text{M}$  using standard methods in the field of biosensing (Lee, 2025).

## 2.3. Cartridge Technology: Microfluidic Sample-Handling

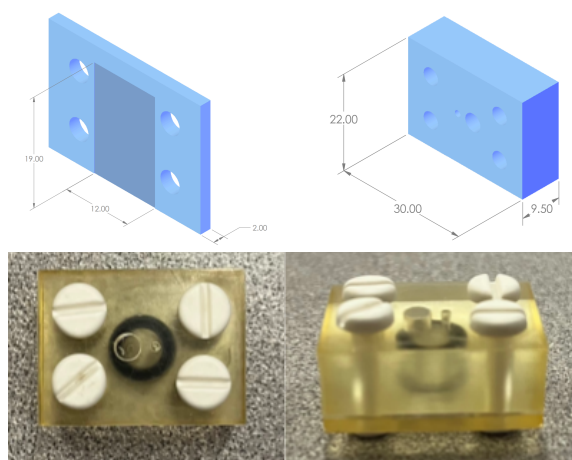


**Fig. 2.** Microfluidic flow cell fabricated for Eindhoven Testing Event. Dimensions in millimeters.

To simulate continuous biosensing in ISF, LIG electrodes fabricated from PI and functionalized as described in Section 2.2 were sized to fit within a 100  $\mu\text{m}$ -deep, 12 x 19 mm slit (Section 8.3). Each electrode connects via extended LIG traces to silver epoxy-coated contact pads outside the slit, enabling Sensit Wearable potentiostat integration while minimizing graphene abrasion. A 100  $\mu\text{L}$  ISF sample is introduced through a 1.5 mm inlet tapering to 1 mm, sealed with the pipette tip to prevent air bubbles. The 58  $\mu\text{L}$  sensing chamber, a circular cavity, is enclosed with a nitrile gasket and secured by four nylon screws. Excess sample exits through a 1 mm outlet into a 75  $\mu\text{L}$  waste reservoir, which flushes residual fluid between measurements.

Inlet and outlet channels are dimensionally matched to promote smooth flow and prevent bubbles. A slight downward slope near the waste vessel reduces backflow and allows clean pipetting of waste without disrupting the flow path, enabling uninterrupted operation (Fig. 2). Creatinine concentration is quantified using four consecutive CV scans per sample; the current response at 84 mV is averaged across scans 2–4 to reduce noise and improve accuracy.

## 2.4. Reader Instrument and User Interaction: Sensit Wearable Potentiostat

The Sensit Wearable potentiostat is used as a stand-in for our custom potentiostat to perform four CV scans per sample. Each scan ranges from -500 to 500 mV at a scan rate of 200 mV/s with a 2.4 mV step size. The algorithm averages the current at 84 mV from scans 2–4 and applies a calibration curve to calculate creatinine concentration (Section 8.4). User interaction is minimal, limited to pipetting samples, exporting CV data from the Sensit, and running a MATLAB script to obtain concentration results. These steps will be automated in the final sensor design.



### 3. IN Award: Biosensor Innovation

#### 3.1. Wearable Sensor

##### 3.1.1. Technological Novelty of Wearable Sensor: Cu-TCPP Metal-Organic Frameworks & Laser-Induced Graphene Transducers

Common creatinine detection methods include isotope dilution-gas chromatography (IDGC) as well as enzymatic assays, such as the Jaffe method. IDGC, commonly referred to as the “gold standard” for creatinine sensing, is expensive and used only in point-of-care (POC) or research environments (Sharma et al., 2022). While some enzymatic assays can be adapted for continuous monitoring, they are often impractical due to the specific storage and operating conditions required for the enzyme(s) to function without denaturing. Furthermore, because creatinine is a relatively small analyte, enzymatic assays are often not specific to its detection, instead detecting any small molecules containing endocyclic nitrogens (Saddique et al., 2023). We chose a chemically tunable, nonbiological recognition element that contains copper ions to be used for continuous sensing of creatinine (Section 8.5).

Creatinine forms complexes with copper ions, a property that enables selective electrochemical monitoring of kidney function through measurement of creatinine concentrations. In ISF, creatinine must first tautomerize through protonation, forming a cyclic double bond that increases its positive charge. This produces an oxidative peak in CV that corresponds to concentration of creatinine based on the number of molecules that tautomerize. However, free copper ions are unstable for long-term *in vivo* use, requiring stabilization within a matrix, such as a MOF.

MOFs are porous, crystalline materials formed from metal ions and organic linkers, offering high surface area and stability (Amali et al., 2022; Cun et al., 2022; Lee & Choi, 2022; Nwosu & Siahrostami, 2023). Copper readily forms complexes with nitrogen- and oxygen-containing ligands due to its vacant d-orbital making it well-suited for MOF integration and inducing binding with creatinine's endocyclic nitrogen. While promising, many MOF-based sensors lack the selectivity and response time needed for continuous *in vivo* monitoring (Alanazi et al., 2025; Ayyandurai et al., 2024; Wu et al., 2022).

Accordingly, we synthesized a Cu-TCPP MOF based on the method of Xu et al., adapting it for continuous and selective creatinine detection (Section 8.2). The Cu-TCPP MOF was suspended in an aqueous Nafion™ solution to enhance stability and electrode compatibility. As shown in Fig. 3b, the Cu-TCPP MOF enables robust creatinine detection, while Nafion™ improves interfacial conductivity and selectively excludes large or negatively charged interferents. At the electrode surface, creatinine becomes protonated, promoting complexation with Cu<sup>2+</sup> ions and producing a measurable redox response via our three-electrode system.

The transduction electrodes were fabricated by functionalizing custom-made LIG, detailed in Sections 2.2 and 8.3. LIG is produced by directly inscribing graphene onto polymers with a commercial CO<sub>2</sub> laser. PI is commonly used for its wide thermal processing window (Ye et al., 2018). This novel process has proved viable in biosensing (Bridges et al., 2025; Chen et al., 2022; Johnson et al., 2021; Shokurov & Menon, 2023; Vivaldi et al., 2021; Zhang et al., 2020). As shown in Fig. 4, LIG can also be

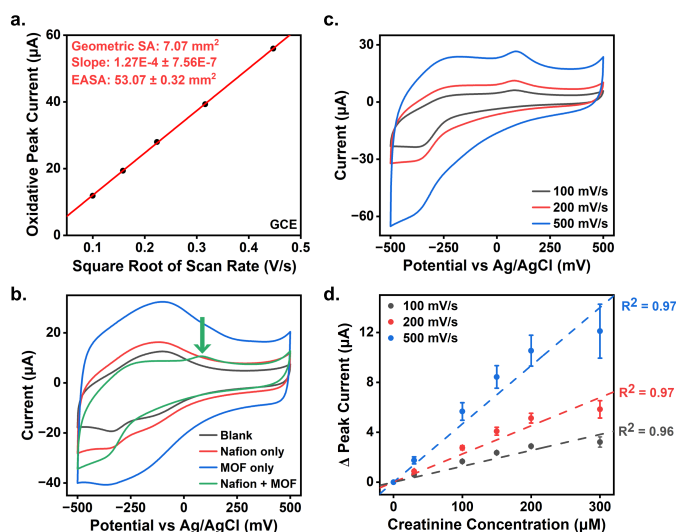


**Fig. 3.** Characterization of Cu-TCPP MOF on GCE. (a) Commercial GCE EASA calculation demonstrates high electroactivity of electrode. (b) CV results of a three-electrode cell in PBS at 150 µM creatinine using four different WE configurations. The presence of an oxidative peak demonstrates Nafion and Cu-MOF to be an effective combination for the detection of creatinine. (c) CV results of three-electrode cell in PBS at 150 µM creatinine using a Nafion + Cu-MOF GCE for the WE and varying scan rates. (d) Calibration curves produced from CV testing at varying scan rates.

derived from SU-8 photoresist, a biocompatible substrate directly patternable onto microneedles (Bachmann et al., 2023). This enables the fabrication of a microneedle-based three-electrode system suitable for wearable biosensing (Section 8.6).

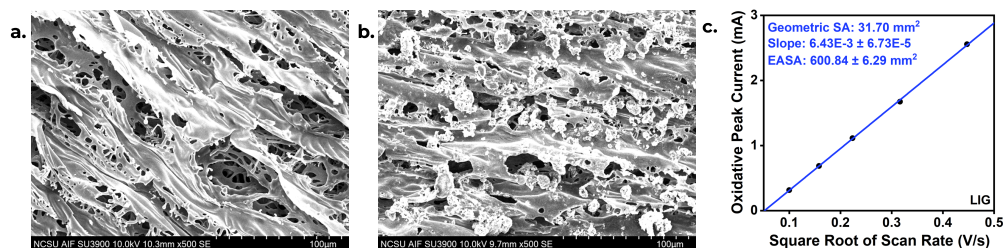


**Fig. 4.** Scanning Electron Microscopy (SEM) imaging of LIG derived from SU-8 that are (a) blank and (b) drop-cast with Cu-TCPP/Nafion suspension. (c) The EASA of one of these LIG electrodes was determined through CV to be  $600.84 \text{ mm}^2$ , aligning with the high porosity demonstrated in SEM images.

### 3.1.2. Technical Feasibility of Wearable Sensor

Before finalizing the wearable sensor design, we optimized the electrochemical conditions for creatinine detection using the Cu-TCPP MOF. As previously demonstrated, the addition of Nafion<sup>TM</sup> solution improved conductivity between the sensing material and electrode surface (Fig. 3). To refine CV parameters — particularly scan rate — we conducted three trials using freshly prepared Cu-TCPP/Nafion<sup>TM</sup> suspensions. Each suspension was drop-cast onto a glassy carbon electrode (GCE), which served as the WE in a three-electrode configuration with a commercial Ag/AgCl RE and platinum (Pt) CE. CV scans were performed at three scan rates across decreasing creatinine concentrations in phosphate-buffered saline (PBS) (Fig. 3c-d). Calibration curves were constructed by averaging current at 84 mV, enabling our MATLAB algorithm to estimate creatinine concentration with minimal error across all tested scan rates (Section 8.4). A 200 mV/s scan rate was selected based on its high accuracy and efficient readout (Fig. 3). Comparable results in buffer and simulated ISF confirm the sensor's selectivity and calibration robustness.

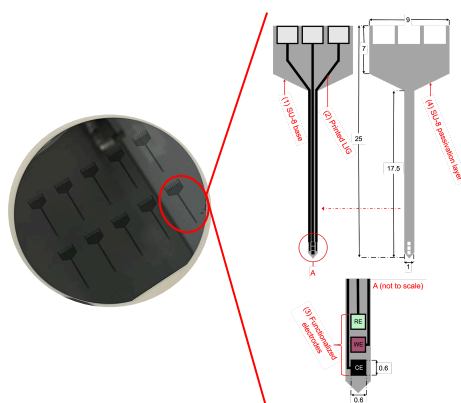


**Fig. 5.** (a) Microneedle production wafer, spin-coated with SU-8. Wafer was produced by Kirstie Queener and Rajendra Shukla. (b) Layered design exposing only the functionalized electrode surfaces and connection pads for potentiostat connection (dimensions in millimeters).

To enable wearability, a patch and applicator system styled after continuous glucose monitors (CGMs) will be adapted to insert an SU-8 based microneedle at a 45° angle to a 0.5-1 mm depth for continuous ISF contact with minimal discomfort. The microneedle consists of four layers: (1) SU-8 base, (2) LIG printed directly onto the SU-8, (3) functional layer with Cu-TCPP/Nafion<sup>TM</sup>, Ag/AgCl, and Pt on the WE, RE, and CE, respectively, and (4) a patterned SU-8 passivation layer exposing only electrode faces and contact pads (Fig. 5). This structural design both protects the graphene electrodes from mechanical and chemical degradation and replicates the flow cell geometry used during the Eindhoven Testing Event (ETE), where reliable creatinine detection in ISF was demonstrated. The microneedle architecture is specifically optimized for electrochemical biosensing and has been validated

across multiple environments, confirming its suitability for continuous analyte monitoring.

In alignment with current CGM benchmarks, the patch-microneedle system is targeting a 10-14 day wear period. A rechargeable, Bluetooth<sup>TM</sup>-enabled potentiostat attaches to the patch via a twist-lock mechanism that connects spring-loaded pins to the microneedle's contact pads. The potentiostat is rated for a three-year lifespan and is reusable across patients, with only the disposable patch and microneedle components requiring replacement. Data is transmitted wirelessly every 15 minutes to a custom mobile application, which calculates real-time creatinine concentrations and glomerular filtration rate (GFR), providing continuous, patient-specific kidney function monitoring (Section 8.7).

## 3.2. Reliability of Sensor Output

### 3.2.1. Technological Novelty of Reliability Concept

**Stability *In Vivo*:** The Cu-TCPP/Nafion™ primary sensing agent enhances long-term biocompatibility and selectivity for creatinine. Free copper ions in ISF can trigger redox reactions and initiate oxidative damage, posing significant health risks. For this reason, copper in the human body is typically bound to enzymes or proteins to avoid such toxicity by immobilizing the copper (Gaetke et al., 2014). Similarly, MOFs entrap copper in a reactive yet stable ionic form through organic linkers. Our Cu-TCPP MOF, composed of the carboxylate-based linker H<sub>2</sub>TCPP and Cu<sup>2+</sup> ions, remains stable in aqueous and mildly acidic environments (Fondo, 2023; Mosca et al., 2023). **By copper colorimetric assay testing, our biosensor exhibited no significant leaching of copper (Section 8.8).** This result is promising for long-term safety *in vivo*.

**Signal Drift and Calibration:** Other than cytocompatibility, the biosensor may lose functionality over time due to changes in conditions, such as ISF acidity or biofouling (Xiang et al., 2025). **As we observed last year, when active copper-binding sites degrade, the CV oxidation peak locations shift. Therefore, peak-to-peak separation is a more reliable indicator of creatinine interaction (Section 8.1).** While this peak shift occurs slowly in our Cu-TCPP MOF, it is still significant. To address this, the sensor takes an initial background measurement shortly after microneedle insertion, assuming a near-fully functional MOF surface. This reading is then compared to the patient's most recent lab creatinine value, allowing the sensor to self-calibrate based on its percent error, which correlates with the viable MOF surface area via a calibration curve. The sensor then reanalyzes the initial data using an updated curve specific to the amount of viable surface area to establish a baseline creatinine level, which can be subtracted from future scans to normalize the data.

**Hardware Reliability:** The LIG electrodes used within our sensor are printed on SU-8, a non-toxic, inert, and flexible substrate that boosts electroactive surface area (EASA) and improves the cost-efficiency of microneedle fabrication (Section 8.3). The miniaturized, Bluetooth™-enabled potentiostat connected to these electrodes via spring-loaded pins further supports wearability through its compact design and long battery life. Paired with a user-friendly mobile interface, it provides patients with real-time access to their creatinine and GFR levels, along with features that simplify kidney health monitoring (Section 8.7).

### 3.2.2. Technical Feasibility of Reliability Concept

The Cu-TCPP MOF demonstrates strong reusability, reliably detecting creatinine across both increasing and decreasing concentration gradients. Due to the bulky nature of our organic linker, Cu<sup>2+</sup>-creatinine coordination complexes are weak and subject to the steric

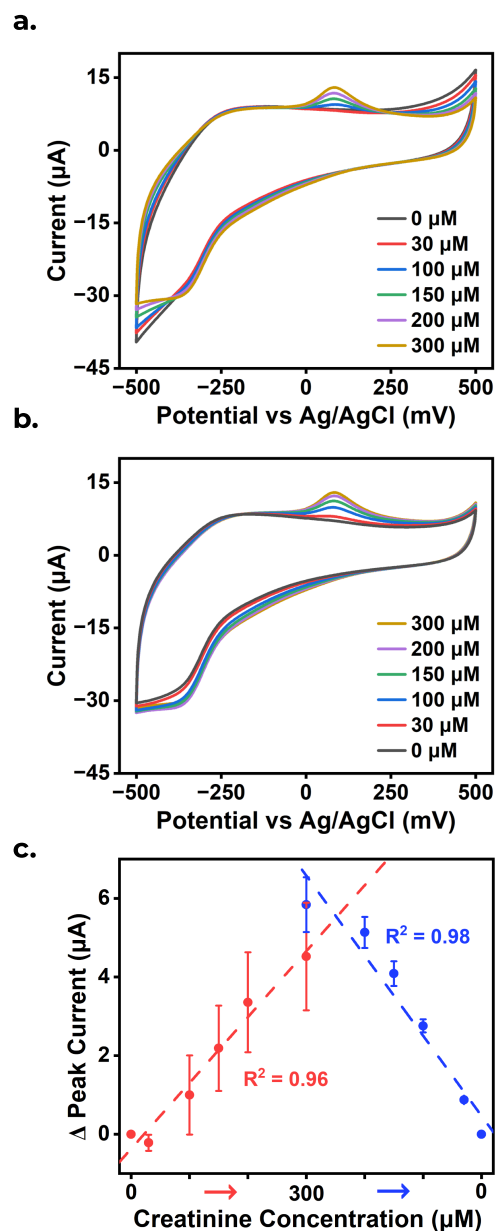


**Fig. 6.** CV performed in PBS using Cu-TCPP MOF/Nafion deposited on a GCE, a Ag/AgCl RE, and Pt CE. Tests were run in incrementally (a) increasing and (b) decreasing creatinine concentrations and (c) calibration curves were formed based on current at 84 mV.

hindrance of the ion. As a result, these complexes can be disrupted by fluid flow as samples of ISF move in and out of the sensing area, ensuring accurate readings regardless of the direction of concentration change (Fig. 6). Like our ETE flow cell design, the wearable will have ISF flowing past the inserted microneedle, continuously breaking and reforming complexes. As the detection of creatinine through ISF is relatively novel compared to blood or urine testing, there is little consensus on lag time of creatinine between blood and ISF. However, glucose lag time has been widely explored and falls between 5-6 minutes (Basu et al., 2015). We expect close to this lag time for creatinine, as it is filtered out of the body similarly to glucose. This verifies our choice of measurement rate (once every 15 min) because it is slower than the estimated lag time for creatinine between blood and ISF. As our sensor is designed to track Post-Operative Acute Kidney Injury (PO-AKI), we anticipate tracking a decrease in creatinine over time except in rare cases, therefore our algorithm uses calibration curves based on CV tests done in decreasing concentrations. These curves better reflect lower concentration changes without sacrificing long-term accuracy. Additionally, in comparing the oxidative current outputs between 0  $\mu\text{M}$  and 30  $\mu\text{M}$  using a paired one-tail t-test, the reported p-value is 0.000195, establishing large statistical significance between the two concentrations. This supports our sensor's ability to accurately detect low concentrations while maintaining a high dynamic range.

As mentioned above, our wearable will be able to self-calibrate, changing the calibration curve in use based on the amount of functional MOF still available. Foundation for this method lies in results from CV testing performed in PBS using Cu-TCPP/Nafion<sup>TM</sup> suspensions that were stored for varying amounts of time deposited on GCEs. Suspensions tested sat out for 1, 4, and 11 days, respectively, to corroborate the reusability of our WE over the suggested minimum insertion period of 10 days for our wearable sensor (Fig. 7). While the performance of the suspension is shown to decrease over time, its functionality remains, as evidenced by the strong, yet variable, trends observed across all suspensions. This enables continuous sensing by allowing us to adjust the method of creatinine concentration calculation to obtain an accurate readout without having to replace any sensor elements for up to 11 days.

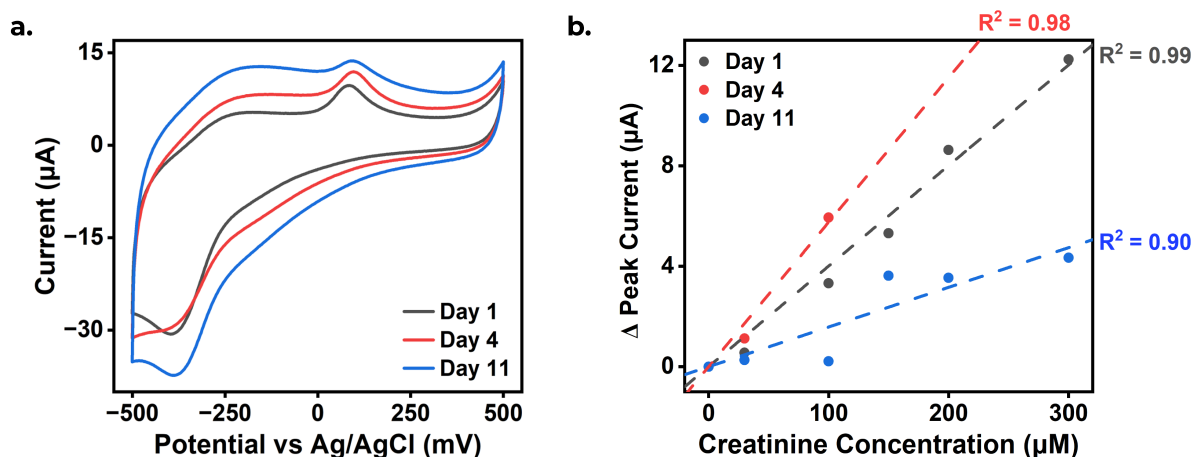


**Fig. 7.** Performance of Cu-TCPP/Nafion suspension over time. (a) CV scans performed in PBS at a creatinine concentration of 150  $\mu\text{M}$ . (b) Calibration curves showing the extended capability of our sensing element to measure creatinine.

To ensure functionality of our sensor, it was also necessary to compare the EASA of our custom LIG electrodes to other commercial electrodes to validate their use as the substrate of our WE (Section 8.3). The LIG electrodes were found to have an amplified EASA compared to a commercially available GCE (Fig. 3). We also quantified the electrochemical behavior of an LIG electrode functionalized with Cu-TCPP MOF/Nafion<sup>TM</sup> suspension drop-cast on its surface to establish the conclusion that our LIG operates within acceptable parameters for the detection of creatinine.

### 3.3. Original Contributions

#### 3.3.1. Team Captains

The SenseNC biosensor introduces a novel, noninvasive method for continuous creatinine monitoring in patients at risk for Post-Operative Acute Kidney Injury (PO-AKI). By enabling earlier detection and intervention, it improves patient outcomes, supports faster recovery, and reduces the risk of complications. Additionally, it allows for earlier discharge, easing hospital capacity, lowering healthcare costs, and saving clinician time. Beyond PO-AKI, the biosensor has strong potential in broader applications, including pediatric kidney care, renal transplant recovery, rural chronic kidney disease (CKD) monitoring, and daily management of CKD.

The core innovation of SenseNC lies in our use of nonbiological creatinine detection through interstitial fluid. Inspired by last year's work, our team selected copper as the sensing element. To address safety concerns such as ion leaching, we conducted an in-depth literature review and developed a copper-based metal-organic framework (MOF), guided by feedback from our supervisor and coaches. We carefully selected synthesis materials and organic linkers to ensure both stability and biocompatibility.

We further enhanced the system by fabricating custom laser-induced graphene (LIG) electrodes, replacing traditional glassy carbon electrodes. This change reduced fabrication time and cost while increasing electroactive surface area - an advantage we plan to leverage in the microneedle-based design of our final product. Using the PalmSens Wearable Potentiostat as a temporary stand-in for our custom potentiostat, we applied voltage sweeps across the LIG electrodes to accurately detect creatinine concentrations via the copper MOF, enabling continuous monitoring without permanent binding to the target molecule. By combining scientific innovation with a robust business strategy - shaped through extensive literature reviews and stakeholder interviews - our team has developed a unique, scalable biosensor with the potential to significantly reduce the burden of PO-AKI and improve kidney care across multiple domains



**Ashley Dehn**

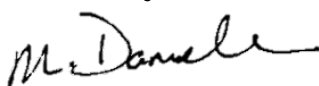


**Charlie Capitano**

#### 3.3.2. Team Supervisor

The SenseNC team developed a novel wearable electrochemical biosensor for continuous creatinine monitoring in ISF, aimed at early detection of PO-AKI. The core innovation lies in the integration of the Cu-TCPP MOF as a non-biological, reversible biorecognition element, directly functionalized onto laser-induced graphene (LIG) microneedle electrodes. This combination leverages copper's selective affinity for creatinine while the MOF structure modulates binding kinetics to enable continuous measurement of both rising and falling concentrations—critical for a true continuous biosensor. Additional design novelties include a permselective Nafion™ layer to enhance specificity and conductivity, a low-dead-volume flow cell compatible with SensUs testing constraints, and a fully integrated wearable potentiostat system with Bluetooth-enabled data transmission and in-app real-time creatinine and estimated GFR calculation.

The students independently identified the MOF-based approach to overcome the stability and specificity limits of last year's copper sensor, adapted synthesis methods, optimized Nafion formulation, engineered the microneedle-flow cell system, and performed electrochemical optimization. My role was limited to ensuring lab access, safety, and providing writing feedback. External contributions were minimal, limited to brief technical training and stakeholder interviews. All major concept selection, design, and testing were conceived and executed by the student team.



**Michael Daniele**



## 4. TP Award: Translation Potential

### 4.1. Customer Interviews

#### 4.1.1. Introduction: Starting with the Patient

Our investigation into unmet clinical needs began by focusing on individuals who have experienced Acute Kidney Injury (AKI), particularly those who developed the condition following surgery or during high-risk hospitalizations. These conversations consistently revealed that AKI is often diagnosed too late, after the patient's condition has already begun to deteriorate. Patients shared the emotional and physical toll of being blindsided by AKI, often describing vague symptoms, a lack of early warning, and the stress of prolonged hospital stays or dialysis.

These discussions strongly informed our choice to target **Post-Operative Acute Kidney Injury (PO-AKI)** as the initial clinical application for our biosensor. According to the American Journal of Kidney Diseases, PO-AKI occurs in approximately 11.8 percent of major surgeries, with even higher incidence in cardiac procedures at 18.7 percent and general surgeries at 13.2 percent (Ayoub et al., 2016). Patients undergoing these surgeries face significantly elevated risks of one-year mortality, with 19 percent mortality among those with AKI compared to 8 percent without, along with long-term consequences including dialysis and end-stage renal disease. This urgency, paired with the absence of a rapid and portable kidney monitoring solution, emphasized the importance of earlier detection and continuous monitoring within the postoperative window.

These interviews helped us reconstruct the PO-AKI patient journey, from initial surgery through hospitalization and discharge. Along that journey, we identified key bottlenecks in care, particularly the lag between physiological kidney injury and its clinical detection. Patients expressed a clear unmet need for earlier, individualized monitoring that could alert providers before symptoms escalate or irreversible damage occurs.

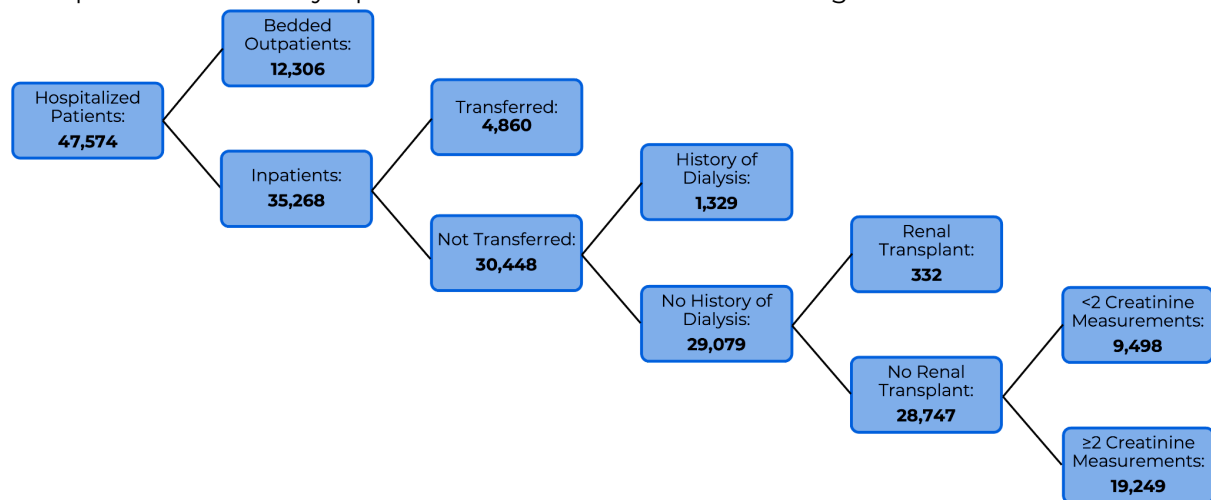


**Fig. 8.** Selection of hospitalized patients eligible for AKI analysis. Of 47,574 total patients, 19,249 met the criteria for AKI detection based on multiple creatinine measurements, highlighting how current diagnosis depends heavily on frequent lab testing. Our biosensor aims to expand AKI detection beyond this limited subset by enabling earlier, more continuous monitoring, especially in patients at risk of being overlooked during short hospital stays or post-discharge (Adapted from Wang et al., 2012).

#### 4.1.2. Healthcare Professionals: Validating Post-Operative Acute Kidney Injury

**To evaluate the clinical relevance and potential impact of a wearable biosensor for continuous creatinine monitoring, we interviewed a total of 16 healthcare professionals. Among them, 8 were nephrologists, 2 were intensive care unit (ICU) nurses, and 6 were other clinicians, including general physicians, intensivists, and anesthesiologists. These interviews included experts from both academic hospitals and community care settings.**

Across disciplines, participants agreed that PO-AKI remains underdiagnosed and poorly addressed, despite its strong association with poor outcomes. A nephrologist from a tertiary-care hospital emphasized that creatinine levels often lag behind real kidney injury, limiting timely intervention. An ICU nurse from a community hospital described

current monitoring as “reactive and infrequent,” noting that kidney deterioration can advance between daily lab draws. A cardiologist echoed these concerns, explaining, “We don’t have any medication that improves kidney function... It’s largely just a wait and see,” highlighting the importance of earlier detection as the primary opportunity for intervention.

There was strong interest in a solution that could provide real-time, non-invasive monitoring. Clinicians expressed that a continuous biosensor could help shift AKI management from reactive to preventive by detecting trends before full renal deterioration. Several also noted the potential to support discharge decisions for patients who are otherwise stable, remarking, “Many times patients are ready to go home, except their creatinine is still high.” ICU nurses in particular emphasized the potential workflow benefits of reducing frequent blood draws and improving patient comfort. Additionally, our choice to sample interstitial skin fluid, which is a clinically accessible and minimally invasive matrix, was seen as compatible with hospital workflows and a promising medium for continuous biomarker monitoring. Several clinicians identified a growing need for post-discharge creatinine monitoring, especially for patients discharged on nephrotoxic medications. Our biosensor offers a potential pathway to bridge inpatient care with outpatient risk surveillance.

#### 4.1.3. Business and Industry Stakeholders: Path to Market

**To develop a feasible roadmap for commercializing our sensor, we conducted 4 interviews with business and industry professionals involved in medical technology, regulatory strategy, and hospital procurement.** These stakeholders offered critical insights into how new biosensing technologies are adopted within healthcare systems. A central theme was that clinical benefit alone is not enough. Successful adoption requires evidence of economic value as well. Metrics like reduced length of stay, with AKI patients averaging 15.8 days compared to 8.6 days for non-AKI patients, lower rates of dialysis, or fewer readmissions, with 21 percent versus 13 percent at 30 days, were cited as compelling business cases for hospital procurement teams. Industry professionals recommended launching in innovation-forward hospital systems and pairing deployment with validation studies that measure both clinical and operational outcomes.

Several stakeholders emphasized the importance of integrating software that improves both clinical decision-making and care coordination. In response to this need, we are developing CreaCare, a companion application that supports real-time creatinine trend monitoring, clinician alerts, and structured patient recovery tracking (Section 8.7). CreaCare displays biosensor readings in a visual dashboard aligned with Kidney Disease Improving Global Outcomes (KDIGO) staging and allows patients to log symptoms, fluid intake, and urination patterns. These features were viewed as especially valuable for assessing discharge readiness and supporting remote monitoring post-discharge. Stakeholders noted that software like CreaCare not only improves usability for providers but also positions the device for smoother workflow integration and future compatibility with electronic health records (EHRs).

From a regulatory standpoint, experts agreed that our device could plausibly qualify as a **Class IIa medical device** under the US Food & Drug Administration and the European Union (EU) Medical Device Regulation (MDR), contingent on rigorous documentation of safety and effectiveness. These interviews shaped the foundation of our early go-to-market strategy and reinforced the importance of aligning user needs, clinical evidence, and commercial feasibility from the outset (Section 8.13).

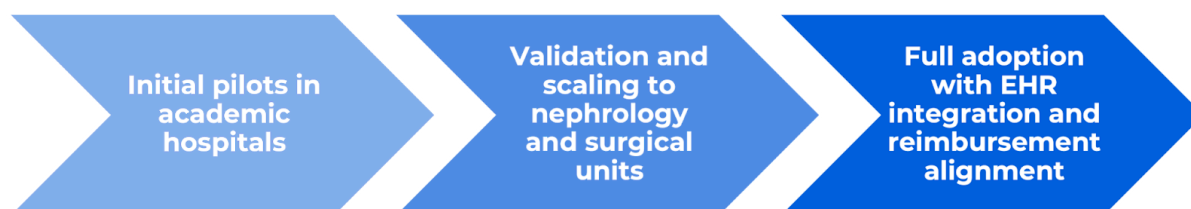


**Fig. 9.** Go-to-market strategy for phased deployment across surgical, nephrology, and outpatient settings.



## 4.2. Design of Validation Study

### 4.2.1. Conceptual Prototype and Relevant Use Case

Fig. 10 shows our 3D-printed conceptual prototype. Computer-aided design (CAD) drawings of the physical sensor and reusable applicator are shown in Appendix 8.9. As discussed in the Section 4.1, PO-AKI patients are an underserved group with high clinical need. Of the 310 million surgeries conducted annually, ~12% result in AKI, equating to roughly 37 million potential cases per year (Dobson, 2020; Liu et al, 2023). Our sensor is designed for

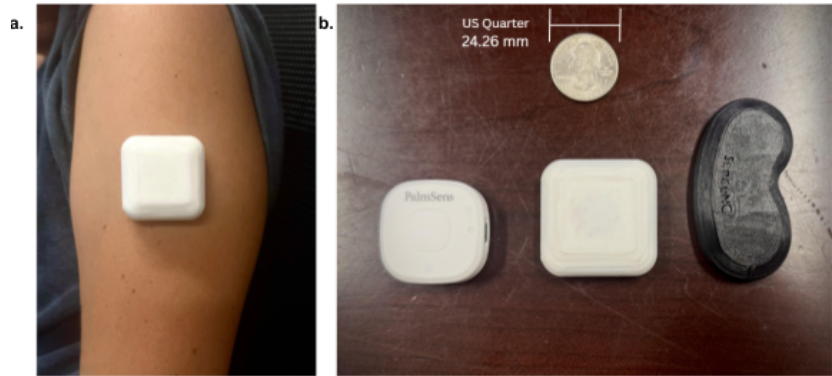


**Fig. 10.** (a) Current sensor design worn on the arm and (b) size comparison between the Palmsens Sensit Wearable (left) and our current sensor design (center). On the right is a shorter, more organically shaped prototype to be paired with a custom potentiostat.

repeated hospital use with the potentiostat component reusable and sterilized between uses per International Organization for Standardization (ISO) Standard 17664 (Processing of Healthcare Products). The device is applied in-hospital using a similarly sterilized applicator, allowing the sensor to be sent home with patients, enabling early discharge when creatinine monitoring is the primary concern. Both patients and clinicians can access real-time data through our companion software, CreaCare, **which will be compatible with EHR systems and have software security measures in place.** Initial testing will focus on device feasibility/reusability, software usability, and cost-effectiveness.

### 4.2.2. Software Usability

To ensure the CreaCare companion app supports both patient recovery and clinical decision-making, a structured usability validation study will be conducted using quantitative metrics and qualitative feedback. Volunteer participants, including patients and providers, will perform predefined tasks such as logging fluid intake, interpreting creatinine trends, and responding to alerts. Evaluators will track usability indicators during the study, including task completion time, number of clicks, and overall success rate.

Following task completion, participants will rate the interface using the 10-item System Usability Scale (SUS), which yields a score between 0 and 100. A score above 80 is considered excellent, while scores below 70 may indicate design usability issues. Additional Likert-style items (1–5 scale) will assess perceived clarity of data presentation, ease of navigation, and the perceived usefulness of app insights. To evaluate cognitive load, we will also administer the National Aeronautics and Space Administration Task Load Index (NASA-TLX), a validated tool for assessing mental demand, temporal demand, and effort. Open-ended responses will be collected to identify usability pain points and suggestions for feature

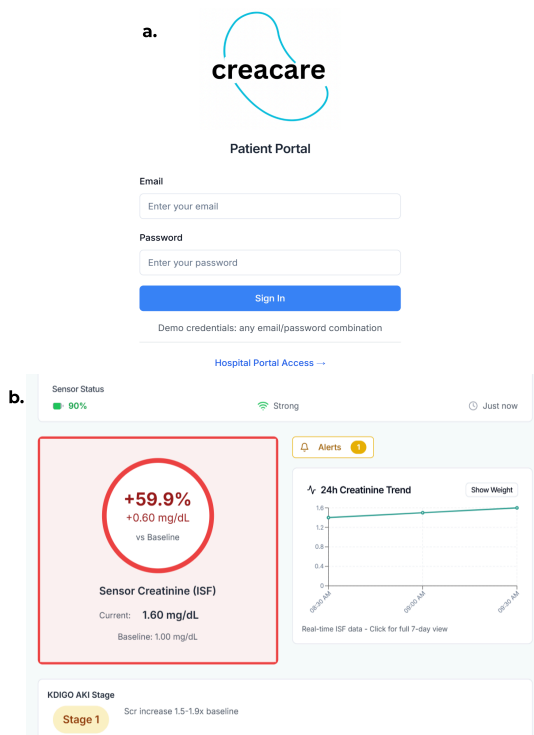


**Fig. 11.** CreaCare software prototype, showing (a) the patient login portal and (b) creatinine monitoring dashboard.

improvement, particularly in areas related to clinician alerting and patient self-tracking.

#### **Target Outcome Metrics:**

Target usability benchmarks include a task success rate above 90 percent, SUS scores exceeding 80, and Likert average ratings above 4.0 for clarity and usefulness. These targets are consistent with benchmarks used in published usability evaluations of mobile tools in nephrology and dialysis care (Reitz et al., 2021). Meeting these standards will demonstrate that the CreaCare platform supports daily engagement, promotes patient adherence, and fits within existing clinical oversight workflows. This study will also serve as a baseline for iterative design improvements and future comparisons with other digital health tools for PO-AKI monitoring.

#### **4.2.3. Device Feasibility and Reusability**

A controlled benchtop study will be conducted to verify safety for future animal trials and to collect preliminary data on the device's accuracy and precision. Simulated interstitial skin fluid (ISF) samples with varying creatinine levels will be applied to eight phantom tissue strips via soaking. Creatinine concentration in each strip will be determined using the gold standard method: isotope dilution-gas chromatography (Sharma et al., 2022). For each trial, one strip is randomly selected and 10 sensors are applied using 10 different reusable applicators. Each sensor operates for 10 days, recording five creatinine measurements daily. One complete trial involves 10 sensors running simultaneously, to be repeated a total of eight times.

The study will evaluate six key device features over the 10-day period: (1) creatinine measurement accuracy/precision compared to gold standard, (2) Bluetooth™ connectivity assessed via average signal strength per applicator per trial, (3) potentiostat battery life recorded at the end of each trial, (4) patch durability monitored throughout the trial with time of failure noted if detachment occurs, (5) applicator usability/reusability evaluated through dye injection and ultrasound imaging of needle tracks, and (6) microneedle injection depth determined from ultrasound images taken daily during each trial.

#### **Target Outcome Metrics:**

The following metrics define success in this study: (1) 95% of a sensor's readings must fall within  $\pm 15\%$  of isotope dilution gas-chromatography values, in line with current CGM requirements detailed in ISO Standard 15197 (*In vitro* diagnostic test systems) (Freckmann et al., 2019). (2) A sensor's average Bluetooth™ signal strength must be between -30 and -65 dBm, with a standard deviation under 15 dB. (3) Battery life of the potentiostat must be above 20% throughout the trial. (4) A patch must remain completely adhered during a 10 day trial. (5) Each applicator must inject all needles to an average depth of 0.5-1 mm with a standard deviation under 50  $\mu\text{m}$  across all trials. (6) A microneedle must remain within 10% of its original depth over the course of a 10 day trial.

Meeting these benchmarks confirms the device's basic safety and performance, allowing progression to animal and clinical trials. As outlined in Section 8.10, subsequent testing in animal and human models will further evaluate sensor performance, safety, and efficacy.

#### **4.2.4. Cost Effectiveness**

As noted in Section 4.2.1., this device targets hospitals to detect an estimated 36 million annual PO-AKI cases. Validating our sensor as a cost-effective home-treatment solution is key to helping hospitals avoid costly overnight stays. To access this large market, our startup plans a conservative U.S. launch, where approximately 45 million major surgeries occur annually and 12% lead to PO-AKI — about 5.4 million cases (Dobson, 2020). We aim to capture 0.09% of this market in year one by producing and selling 5,000 units while additionally accounting for error rates in production. For a full estimation of overhead costs and rationale, see Section 8.11. Additionally, please find our full roadmap to commercial availability in Sections 8.9 through 8.12.

#### **Target Outcome Metrics:**

Accounting for overhead and production errors, the sensor's cost will be set at \$622 — nearly 5 times less than the \$3,025 average cost of a one-night hospital stay in a general U.S. ward (McAllister, 2025).

## 5. Team and Support

### 5.1. Contributions of Team Members

**Dr. Michael Daniele and Dr. Stefano Menegatti** were crucial in the development of our biosensor and business translation efforts. Their support in the process of creating and testing our designs as well as their guidance through technical decisions were necessary for our ability to compete.

**Lina Acosta-Pérez and Irfan Ismail** served as our coaches for this competition, providing invaluable advice and keeping us on track to meet our goals.

**Ashley Dehn** acted as a team captain and head of chemistry, leading weekly meetings and putting in several hours of research and testing. Ashley also assisted with electrical components in the development of the sensor.

**Charlie Capitano** acted as a team captain and head of business, leading weekly meetings and developing the pathway to bring our final sensor design to market. Charlie also heavily contributed to chemistry development.

**Lauren Mabe** acted as the head of electronics/microfluidics, as well as contributing to chemistry and business. Lauren supported both technical development and project management.

**Jenny Lopez** served as a member of the chemistry team, as well as assisting with business and electrical tasks.

**Ameerah Abazid** served as the head of CAD design, as well as contributing to electronics/microfluidics. Ameerah also assisted on chemical synthesis and testing.

**Lily Ro** contributed to chemistry and CAD design, leading much of chemical synthesis. Lily also played a key role in sensor development and led social media content creation.

**Ben Cole** served on the business team and created the project software, managing the app used to support and present our team's biosensor results.

**Jayden Ford** served on the business team, led social media outreach, and contributed to the project's external communication.

### 5.2. People Who Have Given Support

**Kirstie Queener and Rajendra Shukla**, two members of the Biointerface Lab, provided design details for the microneedles and manufactured prototypes, which were adapted for the use of creatinine sensing as detailed in this report.

Several experts and stakeholders provided vital guidance in developing our biosensor. Patients like **Mrs. Bress** and **Mrs. Gilchrist** shared insights into the daily challenges of kidney disease and transplant care, guiding user-centered design. Legal, regulatory, and commercialization input came from **Mr. Wright, Dr. Henderson, Mr. Aaron, and Dr. Hubbard**. Clinical experts—including nephrologists, transplant coordinators, vascular surgeons, and biomedical researchers—highlighted the need for continuous monitoring, especially in pediatric and post-operative care, and advised on clinical integration, usability, and regulatory pathways. See Section 8.13 for individual contributions.

### 5.3. Sponsors and Partners

**NC State Institute for Connected Sensor-Systems (IConS)** and the **NC State Office of Undergraduate Research** provided funding and support for both the development of our biosensor and our travel accommodations.

**DermiSense** provided funding and support for the development of our biosensor.

**NC State College of Engineering** and the **NC State/UNC-CH Lampe Joint Department of Biomedical Engineering** provided funding for our competition travel.

**PalmSens** provided feedback on our electrical and microfluidic components, as well as answered questions about the PalmSens Wearable Potentiostat utilized for the ETE event.

## 6. Final Remarks

We would like to express our sincere gratitude to the patients, clinicians, and industry professionals who generously contributed their time and insights throughout the development of this biosensor. Their lived experiences and professional perspectives were instrumental in shaping a solution that is not only technically robust, but also clinically and emotionally meaningful.

As a student team consisting entirely of undergraduates, we were fortunate to collaborate with mentors and researchers across biomedical engineering, regulatory science, and healthcare delivery. We are especially grateful to the faculty and staff at North Carolina State University and the University of North Carolina at Chapel Hill for providing access to facilities, guidance, and encouragement throughout the SensUs 2025 journey.

Looking ahead, we plan to continue developing our biosensor beyond the competition through institutional support and potential partnerships with clinical and commercial stakeholders. Our immediate goals include refining the hardware for long-term use, expanding validation studies with human-derived ISF, and exploring regulatory submission pathways. We believe that decentralized kidney function monitoring has the potential to improve outcomes for millions of patients, and we are committed to translating this vision into clinical reality.

## 7. References

- Alanazi, A. Z., Alhazzani, K., Ali, A. B. H., Darweesh, M., Ibrahim, H., & El-Wakil, M. M. (2025). Self-Calibrating Copper-Based Metal Organic Frameworks for Ratiometric Electrochemical Sensing of Creatinine. *Electroanalysis*, 37(1), e202400173. <https://doi.org/10.1002/elan.202400173>
- Amali, R. K. A., Lim, H. N., Ibrahim, I., Zainal, Z., & Ahmad, S. A. A. (2022). A copper-based metal-organic framework decorated with electrodeposited Fe<sub>2</sub>O<sub>3</sub> nanoparticles for electrochemical nitrite sensing. *Microchimica Acta*, 189(9), 356. <https://doi.org/10.1007/s00604-022-05450-y>
- Ayoub, I., Almaani, S., Alvarado, A., Parikh, S. V., & Rovin, B. H. (2016). Acute Kidney Injury After Major Surgery: A Retrospective Analysis of Veterans Health Administration Data. *American Journal of Kidney Diseases*, 67(2), A20–A23. <https://doi.org/10.1053/j.ajkd.2015.10.017>
- Ayyandurai, N., Venkatesan, S., & Raman, S. (2024). Palladium Nanoparticle-Decorated Copper-Hemin Metal Organic Framework for Enzymatic Electrochemical Detection of Creatinine in Human Urine. *ACS Applied Bio Materials*, 7(12), 8444–8455. <https://doi.org/10.1021/acsbm.4c01285>
- Bachmann, A. L., Ferris, A. L., Im, S., Dickey, M. D., & Lazarus, N. (2023). Laser-Induced Graphene from SU-8 Photoresist: Toward Functional Micromolding. *ACS Applied Engineering Materials*, 1(1), 222–228. <https://doi.org/10.1021/acsaenm.2c00045>
- Basu, A., Dube, S., Veettil, S., Slama, M., Kudva, Y. C., Peyser, T., Carter, R. E., Cobelli, C., & Basu, R. (2015). Time Lag of Glucose From Intravascular to Interstitial Compartment in Type 1 Diabetes. *Journal of Diabetes Science and Technology*, 9(1), 63–68. <https://doi.org/10.1177/1932296814554797>
- Birdsall, W. J., & Weber, B. A. (1990). Copper(I) and Copper(II) Complexes of Creatinine. *Journal of Coordination Chemistry*, 22(3), 205–208. <https://doi.org/10.1080/00958979009408216>
- Bridges, M., Marin, E., Banik, A., & Henry, C. S. (2025). Simplifying the Incorporation of Laser-Induced Graphene into Microfluidic Devices. *ACS Applied Materials & Interfaces*, 17(22), 32701–32710. <https://doi.org/10.1021/acsaami.5c04078>
- Carroll, D. (2024, December 2). *Calculating the Electroactive Surface Area*. <https://danielpatrickcarroll.substack.com/p/calculating-the-electroactive-surface>
- Chen, B., Johnson, Z. T., Sanborn, D., Hjort, R. G., Garland, N. T., Soares, R. R. A., Van Belle, B., Jared, N., Li, J., Jing, D., Smith, E. A., Gomes, C. L., & Claussen, J. C. (2022). Tuning the Structure, Conductivity, and Wettability of Laser-Induced Graphene for Multiplexed Open Microfluidic Environmental Biosensing and Energy Storage Devices. *ACS Nano*, 16(1), 15–28. <https://doi.org/10.1021/acsnano.1c04197>
- Chen, C., Wang, Z., Chen, G., Zhang, Z., Bedran, Z., Tipper, S., Diaz-Núñez, P., Timokhin, I., Mishchenko, A., & Yang, Q. (2025). Silver Electrodeposition from Ag/AgCl Electrodes: Implications for Nanoscience. *Nano Letters*, 25(23), 9427–9432. <https://doi.org/10.1021/acs.nanolett.5c01929>
- Cun, J.-E., Fan, X., Pan, Q., Gao, W., Luo, K., He, B., & Pu, Y. (2022). Copper-based metal-organic frameworks for biomedical applications. *Advances in Colloid and Interface Science*, 305, 102686. <https://doi.org/10.1016/j.cis.2022.102686>
- Dobson, G. P. (2020). Trauma of major surgery: A global problem that is not going away. *International Journal of Surgery*, 81, 47–54. <https://doi.org/10.1016/j.ijsu.2020.07.017>

- Domínguez-Aragón, A., Conejo-Dávila, A. S., Zaragoza-Contreras, E. A., & Dominguez, R. B. (2023). Pretreated Screen-Printed Carbon Electrode and Cu Nanoparticles for Creatinine Detection in Artificial Saliva. *Chemosensors*, 11(2), 102. <https://doi.org/10.3390/chemosensors11020102>
- Emergo. (n.d.). *FDA Q-Sub Consulting and Pre-Sub Guidance for Medical Devices*. <https://www.emergobyul.com/services/fda-q-sub-consulting-and-pre-sub-guidance-medical-devices>
- European Parliament and the Council of the European Union. (2017). Regulation (EU) 2017/746 of the European Parliament and of the Council. *Official Journal of the European Union*. <https://eur-lex.europa.eu/eli/reg/2017/746/oj/eng>
- Evtugyn, G. (1998). Sensitivity and selectivity of electrochemical enzyme sensors for inhibitor determination. *Talanta*, 46(4), 465–484. [https://doi.org/10.1016/S0039-9140\(97\)00313-5](https://doi.org/10.1016/S0039-9140(97)00313-5)
- Extraspace Storage. (2025). *Raleigh Self Storage at 1515 Sunrise Ave* [Online post]. Extraspace Storage. [https://www.extraspace.com/storage/facilities/us/north\\_carolina/raleigh/7584/](https://www.extraspace.com/storage/facilities/us/north_carolina/raleigh/7584/)
- Fajgenbaum, D. C., & June, C. H. (2020). Cytokine Storm. *New England Journal of Medicine*, 383(23), 2255–2273. <https://doi.org/10.1056/NEJMra2026131>
- Fondo, M. (2023). Copper–Oxygen Compounds and Their Reactivity: An Eye-Guided Undergraduate Experiment. *Journal of Chemical Education*, 100(12), 4791–4795. <https://doi.org/10.1021/acs.jchemed.3c00634>
- Freckmann, G., Pleus, S., Grady, M., Setford, S., & Levy, B. (2019). Measures of Accuracy for Continuous Glucose Monitoring and Blood Glucose Monitoring Devices. *Journal of Diabetes Science and Technology*, 13(3), 575–583. <https://doi.org/10.1177/1932296818812062>
- Gaetke, L. M., Chow-Johnson, H. S., & Chow, C. K. (2014). Copper: Toxicological relevance and mechanisms. *Archives of Toxicology*, 88(11), 1929–1938. <https://doi.org/10.1007/s00204-014-1355-y>
- Gao, J., Hu, Y., Li, S., Zhang, Y., & Chen, X. (2013). Tautomeric equilibrium of creatinine and creatininium cation in aqueous solutions explored by Raman spectroscopy and density functional theory calculations. *Chemical Physics*, 410, 81–89. <https://doi.org/10.1016/j.chemphys.2012.11.002>
- Grieshaber, D., MacKenzie, R., Vörös, J., & Reimhult, E. (2008). Electrochemical Biosensors—Sensor Principles and Architectures. *Sensors*, 8(3), 1400–1458. <https://doi.org/10.3390/s80314000>
- Johnson, E. (2023). NSF 101: America's Seed Fund. *U.S. National Science Foundation*. <https://www.nsf.gov/science-matters/nsf-101-americas-seed-fund>
- Johnson, Z. T., Williams, K., Chen, B., Sheets, R., Jared, N., Li, J., Smith, E. A., & Claussen, J. C. (2021). Electrochemical Sensing of Neonicotinoids Using Laser-Induced Graphene. *ACS Sensors*, 6(8), 3063–3071. <https://doi.org/10.1021/acssensors.1c01082>
- Lee, J. Y., & Choi, J.-H. (2022). Copper-based metal-organic framework for highly efficient adsorption of lead ions from aqueous solution. *Materials Research Express*, 9(9), 095505. <https://doi.org/10.1088/2053-1591/ac93ea>

- Lin, J., Peng, Z., Liu, Y., Ruiz-Zepeda, F., Ye, R., Samuel, E. L. G., Yacaman, M. J., Yakobson, B. I., & Tour, J. M. (2014). Laser-induced porous graphene films from commercial polymers. *Nature Communications*, 5(1), 5714. <https://doi.org/10.1038/ncomms6714>
- Liu, C.-C., Liu, P.-H., Chen, H.-T., Chen, J.-Y., Lee, C.-W., Cheng, W.-J., Chen, J.-Y., & Hung, K.-C. (2023). Association of Preoperative Prognostic Nutritional Index with Risk of Postoperative Acute Kidney Injury: A Meta-Analysis of Observational Studies. *Nutrients*, 15(13), 2929. <https://doi.org/10.3390/nu15132929>
- Liu, H., Xie, Y., Liu, J., Moon, K., Lu, L., Lin, Z., Yuan, W., Shen, C., Zang, X., Lin, L., Tang, Y., & Wong, C.-P. (2020). Laser-induced and KOH-activated 3D graphene: A flexible activated electrode fabricated via direct laser writing for in-plane micro-supercapacitors. *Chemical Engineering Journal*, 393, 124672. <https://doi.org/10.1016/j.cej.2020.124672>
- McAllister, R. (2025, July 2). State-by-State Breakdown—Average Cost of Hospital Stays in the U.S. 2025 [NCHstats]. *North American Community Hub Statistics*. <https://nchstats.com/average-cost-of-hospital-stays-in-us/>
- Ming, P., Niu, Y., Liu, Y., Wang, J., Lai, H., Zhou, Q., & Zhai, H. (2023). An Electrochemical Sensor Based on Cu-MOF-199@MWCNTs Laden with CuNPs for the Sensitive Detection of Creatinine. *Langmuir*, 39(38), 13656–13667. <https://doi.org/10.1021/acs.langmuir.3c01823>
- Mosca, L. P. L., Gapan, A. B., Angeles, R. A., & Lopez, E. C. R. (2023). Stability of Metal–Organic Frameworks: Recent Advances and Future Trends. *The 4th International Electronic Conference on Applied Sciences*, 146. <https://doi.org/10.3390/ASEC2023-16280>
- Nag, A., Mitra, A., & Mukhopadhyay, S. C. (2018). Graphene and its sensor-based applications: A review. *Sensors and Actuators A: Physical*, 270, 177–194. <https://doi.org/10.1016/j.sna.2017.12.028>
- National Archives. (2025). Code of Federal Regulations. *National Archives and Records Administration*. <https://www.ecfr.gov>
- National Library of Medicine. (2025). *ClinicalTrials.gov*. <https://clinicaltrials.gov/>
- Ngamchuea, K., Wannapaiboon, S., Nongkhunsan, P., Hirunsit, P., & Fongkaew, I. (2022). Structural and Electrochemical Analysis of Copper-Creatinine Complexes: Application in Creatinine Detection. *Journal of The Electrochemical Society*, 169(2), 020567. <https://doi.org/10.1149/1945-7111/ac5346>
- Nwosu, U., & Siahrostami, S. (2023). Copper-based metal–organic frameworks for CO<sub>2</sub> reduction: Selectivity trends, design paradigms, and perspectives. *Catalysis Science & Technology*, 13(13), 3740–3761. <https://doi.org/10.1039/D3CY00408B>
- Ostermann, M., Kashani, K., & Forni, L. G. (2016). The two sides of creatinine: Both as bad as each other? *Journal of Thoracic Disease*, 8(7), E628–E630. <https://doi.org/10.21037/jtd.2016.05.36>
- Pacific BioLabs. (2025). *Medical Device Biocompatibility Testing – ISO 10993*. <https://pacificbiolabs.com/biocompatibility>
- Reitz, T., Schwenke, S., Hölzle, S., & Gauly, A. (2021). Usability testing to evaluate user experience on cyclers for automated peritoneal dialysis. *Renal Replacement Therapy*, 7(1), 20. <https://doi.org/10.1186/s41100-021-00340-0>
- Saddique, Z., Faheem, M., Habib, A., UlHasan, I., Mujahid, A., & Afzal, A. (2023). Electrochemical Creatinine (Bio)Sensors for Point-of-Care Diagnosis of Renal



- Malfunction and Chronic Kidney Disorders. *Diagnostics*, 13(10), 1737. <https://doi.org/10.3390/diagnostics13101737>
- SeaCoast Financial, LLC. (2024, October 8). Navigating Healthcare Funding: Grants for Medical Device Development. *Sea Coast Business and Personal Loans*. <https://seacoastloans.com/grants-for-medical-device-development/>
- Sharma, A., Sahasrabudhe, V., Musib, L., Zhang, S., Younis, I., & Kanodia, J. (2022). Time to Rethink the Current Paradigm for Assessing Kidney Function in Drug Development and Beyond. *Clinical Pharmacology & Therapeutics*, 112(5), 946–958. <https://doi.org/10.1002/cpt.2489>
- Shokurov, A. V., & Menon, C. (2023). Laser-Induced Graphene Electrodes for Electrochemistry Education and Research. *Journal of Chemical Education*, 100(6), 2411–2417. <https://doi.org/10.1021/acs.jchemed.2c01237>
- Sigma-Aldrich. (2025). *Copper Assay Kit*. <https://www.sigmaaldrich.com/US/en/product/sigma/mak127>
- Swanson, L. (2025, July 29). Biological Testing Methods of Medical Devices. *NAMSA*. <https://namsa.com/resources/blog/biological-testing-methods-of-medical-devices/>
- The FDA Group. (2024, February 23). A Basic Guide to IQ, OQ, PQ in FDA-Regulated Industries. *The FDA Group*. <https://www.thefdagroup.com/blog/a-basic-guide-to-iq-oq-pq-in-fda-regulated-industries>
- Tsai, K.-Y., Peng, H.-F., & Huang, J.-J. (2023). Nafion modified electrochemical sensor integrated with a feedback-loop indium-gallium-zinc oxide thin-film transistor for enhancing dopamine detection limit. *Sensors and Actuators A: Physical*, 354, 114287. <https://doi.org/10.1016/j.sna.2023.114287>
- U.S. Food and Drug Administration. (2024). *Investigational Device Exemption (IDE)*. <https://www.fda.gov/medical-devices/premarket-submissions-selecting-and-preparing-correct-submission/investigational-device-exemption-ide>
- Vivaldi, F. M., Dallinger, A., Bonini, A., Poma, N., Sembranti, L., Biagini, D., Salvo, P., Greco, F., & Di Francesco, F. (2021). Three-Dimensional (3D) Laser-Induced Graphene: Structure, Properties, and Application to Chemical Sensing. *ACS Applied Materials & Interfaces*, 13(26), 30245–30260. <https://doi.org/10.1021/acsami.1c05614>
- Wang, H. E., Muntner, P., Chertow, G. M., & Warnock, D. G. (2012). Acute Kidney Injury and Mortality in Hospitalized Patients. *American Journal of Nephrology*, 35(4), 349–355. <https://doi.org/10.1159/000337487>
- Wu, N., Guo, H., Peng, L., Chen, Y., Sun, L., Liu, Y., Wei, X., & Yang, W. (2022). Three-step post-synthetic modification metal-organic framework as a ratiometric fluorescent probe for the detection of creatinine. *Microporous and Mesoporous Materials*, 338, 111989. <https://doi.org/10.1016/j.micromeso.2022.111989>
- Xiang, Y., Wei, S., Wang, T., Li, H., Luo, Y., Shao, B., Wu, N., Su, Y., Jiang, L., & Huang, J. (2025). Transformation of metal-organic frameworks (MOFs) under different factors. *Coordination Chemistry Reviews*, 523, 216263. <https://doi.org/10.1016/j.ccr.2024.216263>
- Xu, G., Yamada, T., Otsubo, K., Sakaida, S., & Kitagawa, H. (2012). Facile “Modular Assembly” for Fast Construction of a Highly Oriented Crystalline MOF Nanofilm. *Journal of the American Chemical Society*, 134(40), 16524–16527. <https://doi.org/10.1021/ja307953m>

- Yadav, S., Devi, R., Kumar, A., & Pundir, C. S. (2011). Tri-enzyme functionalized ZnO-NPs/CHIT/c-MWCNT/PANI composite film for amperometric determination of creatinine. *Biosensors and Bioelectronics*, 28(1), 64–70. <https://doi.org/10.1016/j.bios.2011.06.044>
- Ye, R., James, D. K., & Tour, J. M. (2018). Laser-Induced Graphene. *Accounts of Chemical Research*, 51(7), 1609–1620. <https://doi.org/10.1021/acs.accounts.8b00084>
- Zhang, Y., Li, N., Xiang, Y., Wang, D., Zhang, P., Wang, Y., Lu, S., Xu, R., & Zhao, J. (2020). A flexible non-enzymatic glucose sensor based on copper nanoparticles anchored on laser-induced graphene. *Carbon*, 156, 506–513. <https://doi.org/10.1016/j.carbon.2019.10.006>
- Zolotarev, Y. (2025, January 18). How much does it cost to develop medical software in 2025? *Appello*. <https://appello.com.au/articles/how-much-does-it-cost-to-develop-medical-software>

## 8. Appendix

### 8.1. Copper-Creatinine Complexation

Creatinine is a cyclic derivative of creatine that can coordinate with metal ions through lone pair interactions with its nitrogen and oxygen atoms. It is commonly found in two tautomeric forms: amino and imino. In ISF, the amino form, featuring a cyclic secondary amine nitrogen, is more stable. However, metal ions can induce tautomerization in this aqueous environment by facilitating proton transfer from the solution to the creatinine molecule, forming a double bond between the amine nitrogen and an adjacent carbon atom (Fig. 1). This conversion to the imino form enables complexation with metal ions.

As a transition metal,  $\text{Cu}^{2+}$  has vacant d-orbitals that allow coordination with nitrogen and oxygen donor atoms. Infrared (IR) spectroscopy, specifically shifts in the N-H (amino and imino) stretching frequencies, suggest copper binds to the amine nitrogen of creatinine after tautomerization (Birdsall & Weber, 1990). In aqueous environments providing an excess of  $\text{H}_2\text{O}$ , like ISF, copper typically forms a 1:2 complex with creatinine, although a 1:4 binding ratio is also possible (Ngamchuea et al., 2022).

Last year, we leveraged this complexation between copper and creatinine to quantify creatinine concentration in a sample. Copper was electrodeposited on a commercial carbon electrode and used as the WE in a three-electrode electrochemical system for CV testing. In DI water with varying creatinine concentrations, two oxidative peaks were observed (Fig. A1). The first peak, appearing at a lower potential, results from the oxidation of solid copper to  $\text{Cu}^{2+}$ . The second peak, at a higher potential, corresponds to the formation of  $\text{Cu}^{2+}$ -creatinine complexes at the electrode surface.

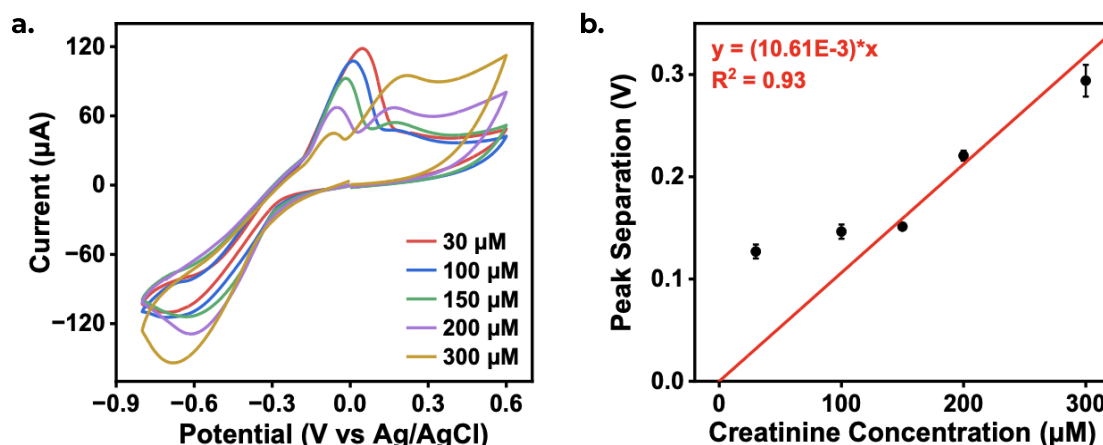


**Fig. A1.** (a) CV results of solid copper in DI water with varying concentrations of creatinine. Results demonstrate (b) a linear relationship between the separation of the two oxidation peaks and creatinine concentration.

This year, we expanded the use of copper's coordination chemistry by developing a copper-based MOF using TCPP organic linkers. These linkers bind  $\text{Cu}^{2+}$  in both 1:2 and 1:4 ratios, reducing available binding sites for creatinine and introducing steric hindrance. We hypothesize that this stable structure prevents irreversible complexation between the creatinine and copper ions. Instead, the ions act as a catalyst, inducing tautomerization at the sensing surface from the amino to the imino form. This tautomerization results in an increase in charge that is detectable through CV and correlates directly to creatinine concentration. We plan to validate this surface tautomerization through Raman spectroscopy, which has been shown to distinguish between creatinine tautomers (Gao et al., 2013).

### 8.2. Synthesis and Deposition of Cu-TCPP Metal-Organic Framework

#### 8.2.1. Chemical Materials

All materials were used as purchased from Sigma-Aldrich without further purification: 0.03 M  $\text{H}_2\text{TCPP}$  (5, 10, 15, 20-tetrakis(4-carboxyphenyl)prophyrin), 0.03 mmol  $\text{Cu}(\text{NO}_3)_2 \cdot 3\text{H}_2\text{O}$  (Copper(II) Nitrate Trihydrate), N,N-Diethylformamide (DEF), and Ethanol Anhydrous.

### 8.2.2. Synthesis of Cu-TCPP MOF

The synthesis of the Cu-TCPP MOF began by preparing a solvent mixture composed of 37.5 mL of DEF and 12.5 mL of ultrapure ethanol, sourced through a nitrogen balloon to minimize the amount of oxygen and water vapor present, resulting in a 75% DEF to 25% Ethanol ratio solution in a 100 mL beaker. Two 24 mL solutions were then prepared in glass vials. The first solution, a 0.01 M solution of  $H_2TCPP$ , was made by weighing out approximately 189.8 mg and then dissolving it in 24 mL of DEF/ethanol solvent mixture. The second solution, a 0.01 M solution of  $Cu(NO_3)_2$ , was prepared by weighing out 57.9 mg and dissolving it in 30.88 mL of the same DEF/ethanol mixture. The Teflon® liner, used in the autoclave, was rinsed with the remaining DEF/ethanol mixture to ensure complete transfer to the interior of the liner. 10 mL of each solution was combined into the Teflon® liner of a 25 mL autoclave. The autoclave was then carefully assembled, sealed, and placed in an oven at 80°C for 24 hours. The mixture was then removed from the oven and left to cool to room temperature for 11 hours.

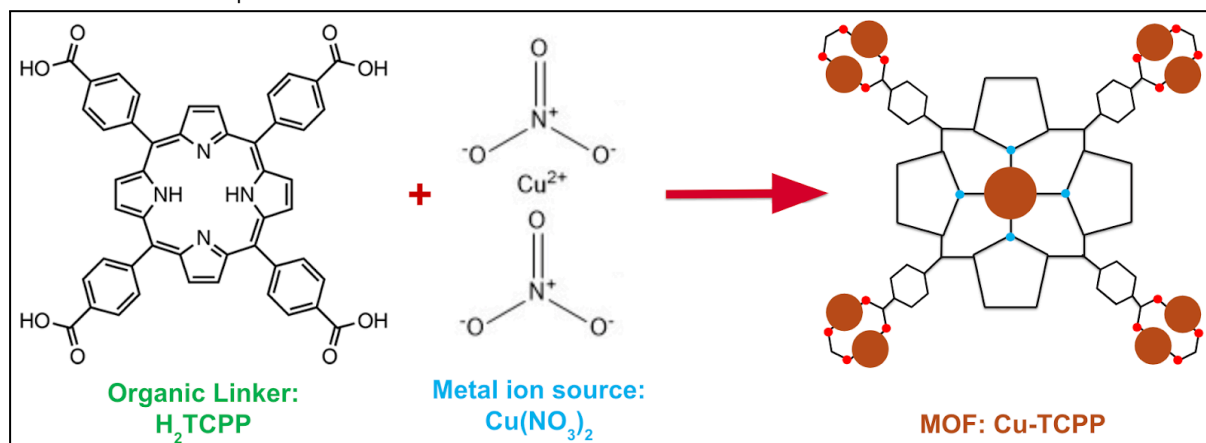


**Fig. A2.** Chemical Synthesis of Cu-TCPP MOF.

### 8.2.3. Cu-TCPP MOF Separation

Following MOF synthesis, the separation and washing procedure began by pouring the solution from the autoclave into two separate 15 mL test tubes using a funnel, ensuring that as close to a 50/50 split as possible to balance on a centrifuge. The funnel and autoclave were rinsed with pure ethanol for any remaining solution and the final volume was adjusted. The tubes were then vortexed for 10 seconds to mix in a significant amount of powder. The tubes then proceed with a series of centrifugation steps (30 minutes apiece), with varying amounts of pure ethanol added and mixed between each spin. The goal throughout was to wash the samples thoroughly and remove as much DEF as possible, leaving behind only ethanol and solid powder. Two mL of ethanol were added to each tube and vortexed once more before transferring all contents to a glass petri dish, the dish is then left in a 60-80 °C oven overnight. The petri dishes were removed from the oven and powder was scraped off with a razor blade (Fig. A3).

### 8.2.4. Cu-TCPP MOF Suspension

MOF was measured out and suspended in solvent at a 2:1 ratio of MOF to liquid. The solvent was prepared using a mixture of Nafion™ and MilliQ water at a 1:20 ratio. The mixture was then ultrasonicated for 35 minutes at an amplitude of 40 microns to achieve a stable colloidal suspension. The colloidal suspension was verified via the

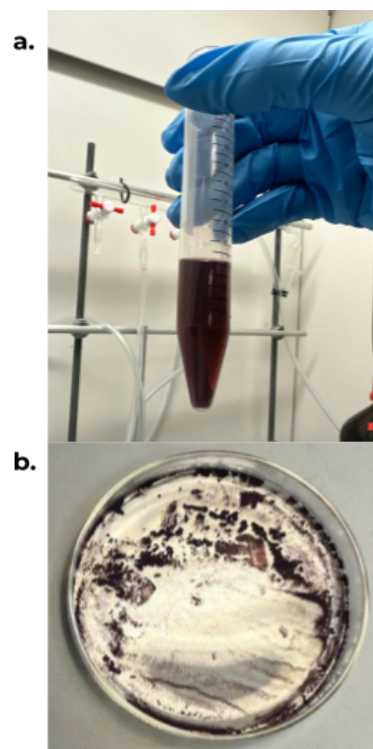


**Fig. A3.** (a) Partly washed MOF solution collected from autoclave following synthesis and (b) washed and dried MOF powder final product

Tyndall effect, which showed light became visible when passed through the even suspension of particles (Fig. A4).

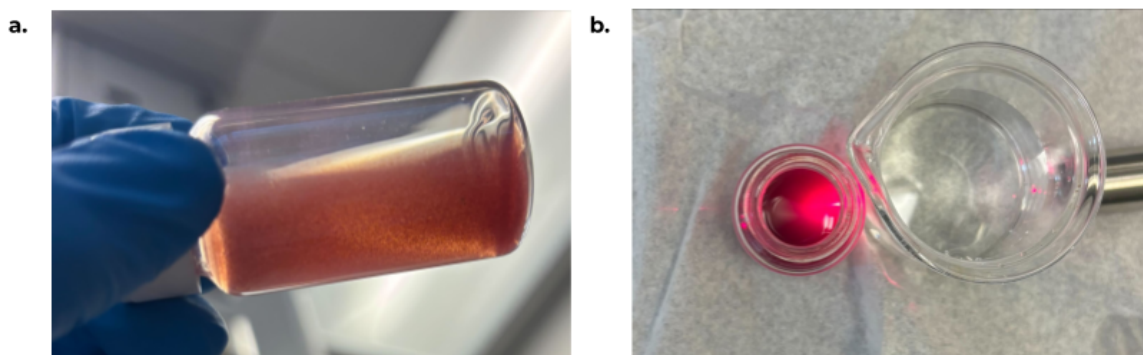


**Fig. A4.** (a) Colloidal suspension of Cu-TCPP MOF in MilliQ and Nafion™. (b) Colloidal suspension was verified via the Tyndall effect.

### 8.2.5. Thin Film Deposition

This stamping method involved forming thin film sheets of the colloidal suspension of the MOF on the surface of a water-filled beaker. This was done by drop-casting the suspended MOF solution onto the surface of DI water (Fig. A5). The clean electrode surface was then gently pressed onto the film, enabling the transfer of the material from the water surface onto the solid support in a stamp-like manner. This technique allowed for the formation of uniform and controlled orientation of the transfer of material (Xu, 2012).

### 8.2.6. Drop-Casting

Although we initially tried using the thin film deposition method detailed in Section 8.2.5, we found this technique was not ideal for depositing our desired concentration onto the electrode surface. Instead, we used a similar deposition method in which a known volume of the MOF suspension is directly pipetted onto the target electrode. For the Cu-TCPP MOF, 5  $\mu$ L of the suspension were added then dried at 80 degrees for approximately 5 minutes. This step was repeated once more to build up the film, resulting in a total of 10  $\mu$ L deposited. This method creates a thicker and more concentrated film which is beneficial when a higher amount of active material is needed on the electrode.

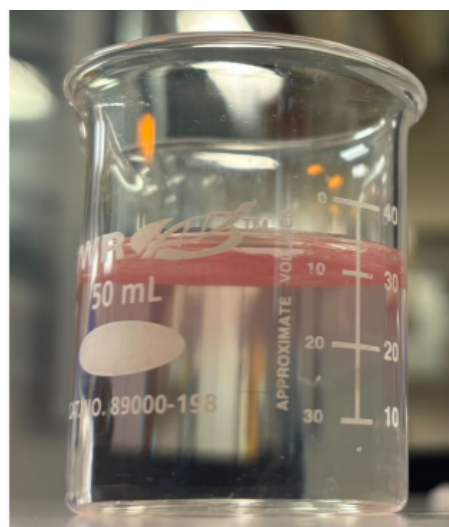


**Fig. A5.** Cu-MOF suspended in ethanol and drop-cast onto surface of DI water.

## 8.3. Laser-Induced Graphene Production and Characterization

### 8.3.1. LIG Formation on PI and SU-8

Graphene is a highly conductive carbon allotrope consisting of a 2D hexagonal lattice, allowing for impressive flexibility and mechanical strength in addition to desirable electrical properties (Nag et al., 2018). While this material can be produced utilizing several methods, such as mechanical exfoliation of graphite, thermal decomposition and reduction of graphene oxide, or chemical vapor deposition, these methods are time-intensive, complicated, and expensive, marking laser irradiation as a cheap and efficient alternative (Vivaldi et al., 2021). Using a polymeric substrate, laser irradiation employs a photothermal reaction to convert the  $sp^3$ -hybridized carbon within the polymer into  $sp^2$ -hybridized carbon (Lin et al., 2014). However, this laser-induced graphene (LIG) deviates from graphene's usual structure, forming a 3D porous, hybrid lattice of 5- and 7-membered rings. This lattice, termed "kinetic graphene," forms due to rapid cooling following the localized high temperature and pressure of laser irradiation, leading to an



inhomogeneous structure whose topology and properties can be tuned through the laser settings (Ye et al., 2018).

As such, our team utilized 120 micron sheets of PI, a commonly used polymer for LIG production, as our initial substrate. To prep the polymer, the sheet was cut to the desired size, the surface was cleaned with isopropyl alcohol (IPA), and the sheet was taped to an acrylic base in order to prevent deformation during irradiation. To inscribe graphene, a commercial CO<sub>2</sub> laser (Glowforge Pro) was used, allowing for speed, power, lines per inch, number of passes, and other settings to be optimized for conductivity. As such, we utilized a speed of 600, 80% power, and 340 lines per inch when “engraving” LIG onto the PI surface. These settings allowed for thick LIG lattices to form, with higher density lines created directly under the laser’s path. A similar effect can be seen when printing on SU-8, a photoresist spin-coated onto silicon wafers (Bachmann et al., 2023). Due to a difference in the properties of PI and SU-8, the laser settings were re-optimized to a speed of 500, 25% power, and 1355 lines per inch, which also increases porosity in this new substrate (Fig. A6). This increased porosity allows a more seamless integration with Cu-TCPP MOF compared to PI, increasing signal strength and supporting our use of SU-8 in our microneedle design & production (Section 8.6).

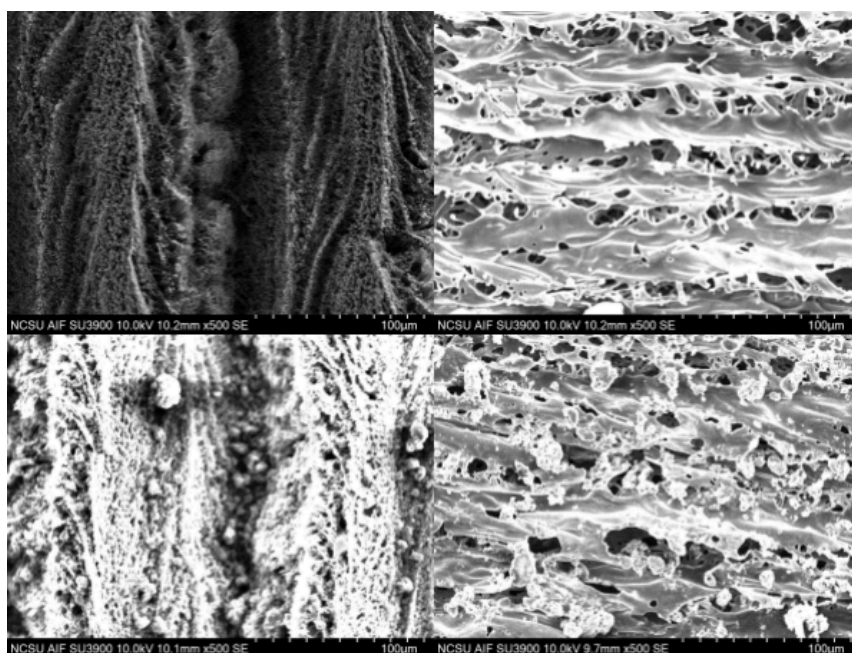


**Fig. A6.** Scanning Electron Microscope (SEM) images of LIG printed on PI (top left), LIG printed on SU-8 (top right), PI LIG drop-casted with Cu-TCPP MOF (bottom left), and SU-8 LIG drop-casted with Cu-TCPP MOF (bottom right).

### 8.3.2. Electrode Fabrication for ETE Event

To fabricate a three-electrode system in which to insert into our Flow Cell designed for the ETE (Section 2.3), our team opted for the efficient and effective fabrication of LIG on PI (Section 8.3.1). As shown in Fig. A7, three LIG electrodes were printed onto PI and functionalized as described in Section 2.2. The three electrode faces are designed to maximize EASA within the gasket-sealed sensing area, with the middle electrode drop-casted with Cu-TCPP MOF, the right electrode electroplated with Ag/AgCl (Chen et al., 2025), and the left electrode remaining unfunctionalized. This procedure is designed to simulate the similar design of our microneedle, with the exception of the PI substrate.

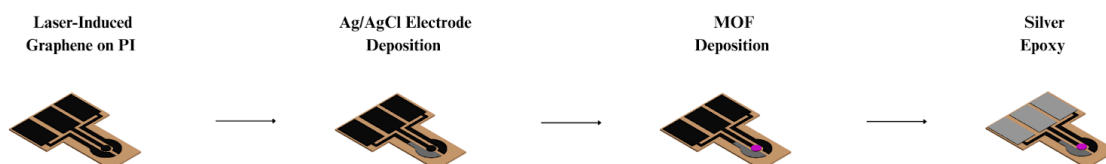


**Fig. A7.** PI-based LIG electrodes to be used at the Eindhoven Testing Event. Includes a Ag/AgCl electroplated RE, a Cu-TCPP MOF deposited WE, and a bare graphene CE.

### 8.3.3. EASA Characterization

To verify the use of LIG electrodes, their EASA was characterized and compared to commercially available electrodes using a modified version of the Randles-Sevcik equation, displayed below:

$$EASA = \frac{m}{(2.69 \times 10^5) \cdot n^{3/2} \cdot A \cdot D^{1/2} \cdot C}$$

The variable  $m$  refers to the slope of the graph of oxidation peak current (amps) over the square root of the scan rate (V/s),  $EASA$  refers to the electroactive surface area ( $\text{cm}^2$ ),  $A$  refers to the geometric surface area ( $\text{cm}^2$ ),  $n$  refers to the amount of electrons transferred in the redox system,  $D$  refers to the diffusion coefficient for the redox probe ( $\text{cm}^2/\text{s}$ ), and  $C$  refers to the concentration of the redox species ( $\text{mol}/\text{cm}^3$ ) (Carroll, 2024). In these experiments, potassium ferrocyanide was used as the redox probe, dissolved in a PBS solution with 0.1 M KCl as a supporting electrolyte, yielding a diffusion coefficient of  $6.3\text{E-}6 \text{ cm}^2/\text{s}$  (Liu et al., 2020). As such, only one electron is transferred in our redox system ( $n$ ). In comparing different commercially available electrodes, including gold, glassy carbon, and screen-printed carbon electrodes, to our LIG electrodes, we saw a major increase in EASA in respect to geometric surface area, supporting our use of LIG (Fig. A7 ; Fig. A8).

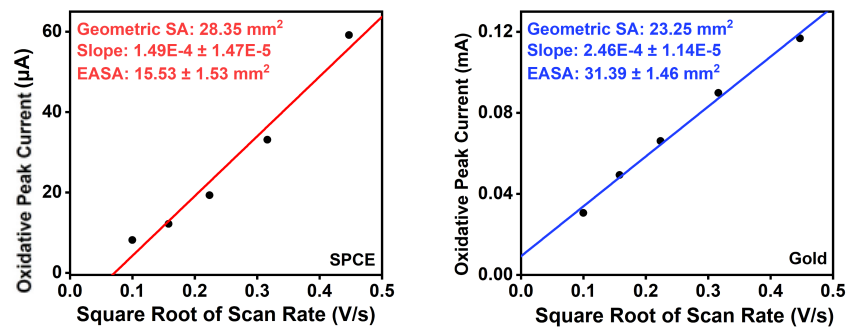


**Fig. A8.** EASA characterization of commercially available gold (left) and screen-printed carbon (right) electrodes.

### 8.4. Creatinine Concentration Algorithm

To calculate creatinine concentration from CV data, we use a set of MATLAB algorithms that average the current response at a set potential and apply a calibration curve to determine creatinine concentration. Before testing unknown samples, a calibration run is performed using ISF with no creatinine to establish the baseline current at 84 mV, which was identified as the stable peak location for creatinine oxidation. The baseline current is obtained using our first MATLAB script, which processes the uploaded potential and current data from the WE (Fig. A9). To reduce noise, the script averages current across scans 2-4, excluding the unstable first scan, and then extracts the average current at 84 mV.

```
%% ETE_FindBase_SensUs2025
clear
clc
close all
%% Declarations / Data Upload
peak_Pot = 0.083738327; %[V] Creatinine
oxidation peak location
data = xlsread('0Scans_ETE.xlsx');
potential = data(:, 4);
current = data(:, 3);
scan_Num = data(:, 5);
%% Separating Scans
s2l = scan_Num == 2;
s2_Cur = current(s2l);
s2_Pot = potential(s2l);
s3l = scan_Num == 3;
s3_Cur = current(s3l);
s3_Pot = potential(s3l);
s4l = scan_Num == 4;
s4_Cur = current(s4l);
s4_Pot = potential(s4l);

%% Eliminating Reduction (Bottom) Half of CV
pos1 = s2_Cur > 0;
s2_Cur = s2_Cur(pos1);
s2_Pot = s2_Pot(pos1);
s3_Cur = s3_Cur(pos1);
s3_Pot = s3_Pot(pos1);
s4_Cur = s4_Cur(pos1);
s4_Pot = s4_Pot(pos1);
%% Averaging Scans
pot = mean([s2_Pot, s3_Pot, s4_Pot], 2);
cur = mean([s2_Cur, s3_Cur, s4_Cur], 2);
%% Determining 0 Baseline Value
[~, i] = min(abs(pot - peak_Pot));
peak_Cur = cur(i);
%% Reporting Results
fprintf('Current at 0 uM Creatinine: %+.6e\n', peak_Cur);
```

**Fig. A9.** MATLAB algorithm used during ETE to calculate current value in a sample of ISF containing no creatinine for normalization.



The baseline current is then used by a second MATLAB script to normalize CV data from unknown samples, enabling use of our calibration curve equation (Fig. A10). After running an unknown sample through CV, data from four scans is uploaded in a spreadsheet and scans 2-4 are once again average to reduce noise. Then, the baseline current from the blank sample is subtracted from all current values. The resulting normalized current at 84 mV is plugged into the calibration curve equation to calculate creatinine concentration. This two-step algorithm enables easy updates to the calibration equation based on the MOF's performance at the WE surface, a feature that would be automated in our final wearable sensor design.

```

%% ETE_Samples_SensUs2025
clear
clc
close all
%% Declarations / Data Upload
peak_Pot = 0.083738327; %(V)
Creatinine oxidation peak location
baseline_Cur = 4; %(A) Obtained
from blank calibration sample
data =
xlsread('Sample#_ETE.xlsx');
potential = data(:, 4);
current = data(:, 3);
scan_Num = data(:, 5);

%% Separating Scans
s2I = scan_Num == 2;
s2_Cur = current(s2I);
s2_Pot = potential(s2I);
s3I = scan_Num == 3;
s3_Cur = current(s3I);
s3_Pot = potential(s3I);
s4I = scan_Num == 4;
s4_Cur = current(s4I);
s4_Pot = potential(s4I);

%% Eliminating Reduction
(Bottom) Half of CV
posI = s2_Cur > 0;
s2_Cur = s2_Cur(posI);
s2_Pot = s2_Pot(posI);
s3_Cur = s3_Cur(posI);
s3_Pot = s3_Pot(posI);
s4_Cur = s4_Cur(posI);
s4_Pot = s4_Pot(posI);

%% Averaging Scans &
Normalizing Current to Baseline
Value
pot = mean([s2_Pot, s3_Pot,
s4_Pot], 2);
cur = mean([s2_Cur, s3_Cur,
s4_Cur], 2);
cur = cur - baseline_Cur;
%% Determining Current at Peak
Potential
[~, I] = min(abs(pot - peak_Pot));
peak_Cur = cur(I);
%% Relating Current to Creatinine
Concentration
creat_Con = peak_Cur / (2.26E-8);
%% Reporting Results
fprintf('Peak Current: %+.6e\n',
peak_Cur);
fprintf('Creatinine Concentration
(uM): %f\n', creat_Con);

```

**Fig. A10.** MATLAB algorithm used during ETE to determine creatinine concentration of unknown samples.

## 8.5. Comparison of Creatinine Detection Methods

**Table A2.** Comparison of dynamic ranges and sensitivities of existing creatinine biosensors to our Cu-TCPP MOF-based biosensor.

Creatinine Measurement Method	Sensitivity (A/M)	Dynamic Range (M)	Source
Cu-TCPP MOF	0.027	0–230	Our sensor
CuNPs/Cu-MOF199@MWCNTs/GCE	1.88	0.05–40.0	(Sung Min et al., 2024)
PTSPCE/CuNPs	0.258	10–160	(Domínguez-Aragón et al., 2023)
ZnO/chitosan/carboxylated MWCNT/polyaniline	0.030	10–650	(Yadav et al., 2011)

## 8.6. Microneedle Design and Production

To allow flexibility in the manufacturing process, our team formulated three possible microneedle designs (Fig. A11). The first was a microneedle made of SU-8 with LIC electrodes printed on the surface. Cu-TCPP MOF would be drop-cast on the WE, Ag/AgCl would be electroplated on the RE, and the CE would be left as bare graphene. Another layer of SU-8 would cap the microneedle, leaving just the functionalized electrode faces exposed. The microneedle would be inserted into the skin using a hollow needle applicator and would remain in the body for a 10-day period, similar to current CGM systems. We adapted this design from experienced researchers in the BioInterface Lab (Section 5.2), ensuring the safety of SU-8 within the body and validating the manufacturing method. As such, we decided to move forward with this design as our most promising method.

The second idea was to have an array of hollow silicone microneedles that utilize capillary action to bring ISF up through a microfluidic system where the electrodes will be located. The ISF would then be discarded into a waste chamber that is located in the wearable device. We decided against this idea since a waste chamber would add weight to the device, creating possible complications in adhesion and leakage.

The third design was a thin microneedle with six layers, similar to those found in CGMs. The innermost layer will contain a gold wire base, on which our Cu-TCPP MOF will be drop-cast. It is then dipped in a capping layer, leaving the bottom 1 mm uncapped. The next layer, starting 0.1 mm after the initial capping, is an Ag/AgCl layer. The second capping layer leaves 1 mm of the silver exposed. The final platinum layer leaves 2 mm

exposed after the final capping. This style, inspired by the Dexcom CGM, requires precise dipping, ensuring that there is no interference between the electrodes. It also requires handling liquid metals which is more dangerous and not as cost effective as the first design.

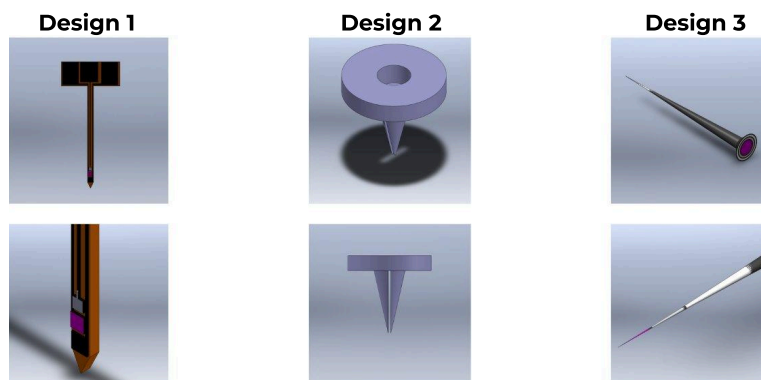


**Figure A11.** Our three microneedle design options, including our chosen design (Design 1).

## 8.7. Companion Software: CreaCare

### 8.7.1. App Functionality and Features

The CreaCare companion application is designed to support both patients and providers through real-time kidney health monitoring and recovery tracking. On the patient side, the app enables users to log daily fluid intake, urination patterns, and symptoms such as fatigue, nausea, or confusion. Patients can also view simplified creatinine trends, receive personalized reminders, and access educational materials that reinforce adherence. A built-in alert system notifies patients if readings exceed pre-set thresholds, prompting early contact with clinicians (Fig. A12).

**Patient Profile:**

**Jane Smith**  
 Patient ID: CF-2024-001  
 Last Updated Today, 2:30 PM  
 Female Age 55 Post-Op Day 3

**Pre-Operative Baseline**

Kidney Function	Surgery Details
Pre-op Serum Creatinine: 1 mg/dL	Procedure: Laparoscopic Colorectal Resection
Pre-op eGFR: 75 mL/min/1.73 m <sup>2</sup>	Date & Time: November 15, 2025, 08:30 AM
Comorbid CKD: Stage 2	Duration: 4.5 hours
	Intra-op Hypotension: 2 episodes

**Demographics & Current Vitals**

Date of Birth	Height	Weight
March 15, 1970	5'6"	154 lbs (70 kg)
BMI: 24.8	Blood Pressure: 138/85	Heart Rate: 78 bpm

**Daily Recovery Log**

Daily monitoring helps your care team track your kidney recovery. Please report any symptoms and record your fluid intake and voiding frequency.

**Total Fluid Intake (Last 24 Hours)**

Total fluids consumed (mL): 1500

Include all beverages: water, juice, coffee, tea, soup, etc.

**Urination Frequency**

☐ I have urinated ≥ 3 times in the last 8 hours

Normal urination frequency indicates healthy kidney function and adequate hydration.

**Sensor Status**

☐ Sensor patch is loose or has come off

**Post-Operative Symptoms**

☐ Sudden weight gain  
☐ Peripheral edema (swelling)  
☐ Dyspnea (shortness of breath)  
☐ Nausea/Vomiting  
☐ Confusion  
☐ Muscle cramps  
☐ Flank pain  
☐ Other

**Additional Notes**

Any other concerns or observations about your recovery...

**Fig A12** CreaCare patient portal, showing patient profile (left) and daily recovery log (right).

For clinicians, the hospital portal provides a centralized dashboard with real-time biosensor data visualized against KDIGO staging criteria. Providers can monitor multiple patients simultaneously, with flagged alerts for critical creatinine trends, missed logs, or changes in symptoms. Key interface components include a patient overview table, detailed creatinine trend graphs, post-operative day tracking, and direct links to view patient histories (Fig. A13). Integrated filters support case prioritization, while quick-access tools allow providers to generate reports or initiate patient contact. All features are designed to function seamlessly within existing electronic health systems with minimal training.

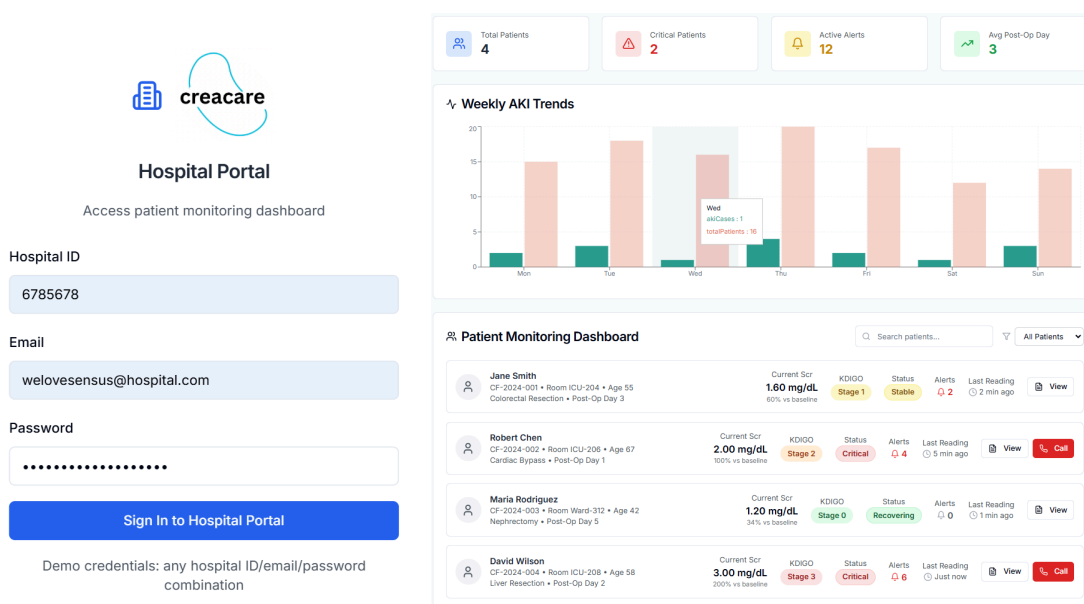


**Fig. A13.** CreaCare doctor portal, showing login section (left) and hospital dashboard (right)

### 8.7.2. Clinical and Operational Value to Hospitals

CreaCare addresses a significant gap in postoperative care by enabling proactive, data-driven monitoring of patients at risk for Acute Kidney Injury (AKI). By streamlining creatinine tracking and reducing dependence on daily blood draws, the app can facilitate earlier discharge for stable patients and reduce hospital length of stay. In the inpatient setting, the app's clinician dashboard enhances workflow efficiency by consolidating relevant metrics into a single interface, allowing faster decision-making and more targeted rounding.

The system also supports remote monitoring post-discharge, which is particularly valuable for patients discharged on nephrotoxic medications or living in rural areas. Stakeholders have emphasized the app's potential to reduce readmissions, improve patient satisfaction, and enhance continuity of care. By aligning with hospital performance metrics such as reduced dialysis incidence and shorter average stays, CreaCare contributes to both clinical quality goals and cost-effectiveness targets. Its modular design further supports long-term integration with hospital electronic health records, increasing its adaptability for future expansion.

### 8.8. Colorimetric Copper Assay for Evaluation of $\text{Cu}^+$ and $\text{Cu}^{2+}$ Leaching

We used the Sigma-Aldrich Copper Assay Kit (MAK127) to test whether our Cu-TCPP MOF releases free copper ions under aqueous conditions. The kit detects  $\text{Cu}^{2+}$  through a chromogenic reaction with absorbance measured at 359 nm (Sigma-Aldrich, 2025). Instead of testing the MOF as a suspension, we dried it onto a surface and then added PBS to better reflect how the MOF would behave once coated on a device and exposed to fluid. After letting the PBS sit in contact with the dried MOF, we collected the solution and ran the test using a 96-well plate. A water blank and a 300  $\mu\text{g}/\text{dL}$  copper standard were included for comparison.

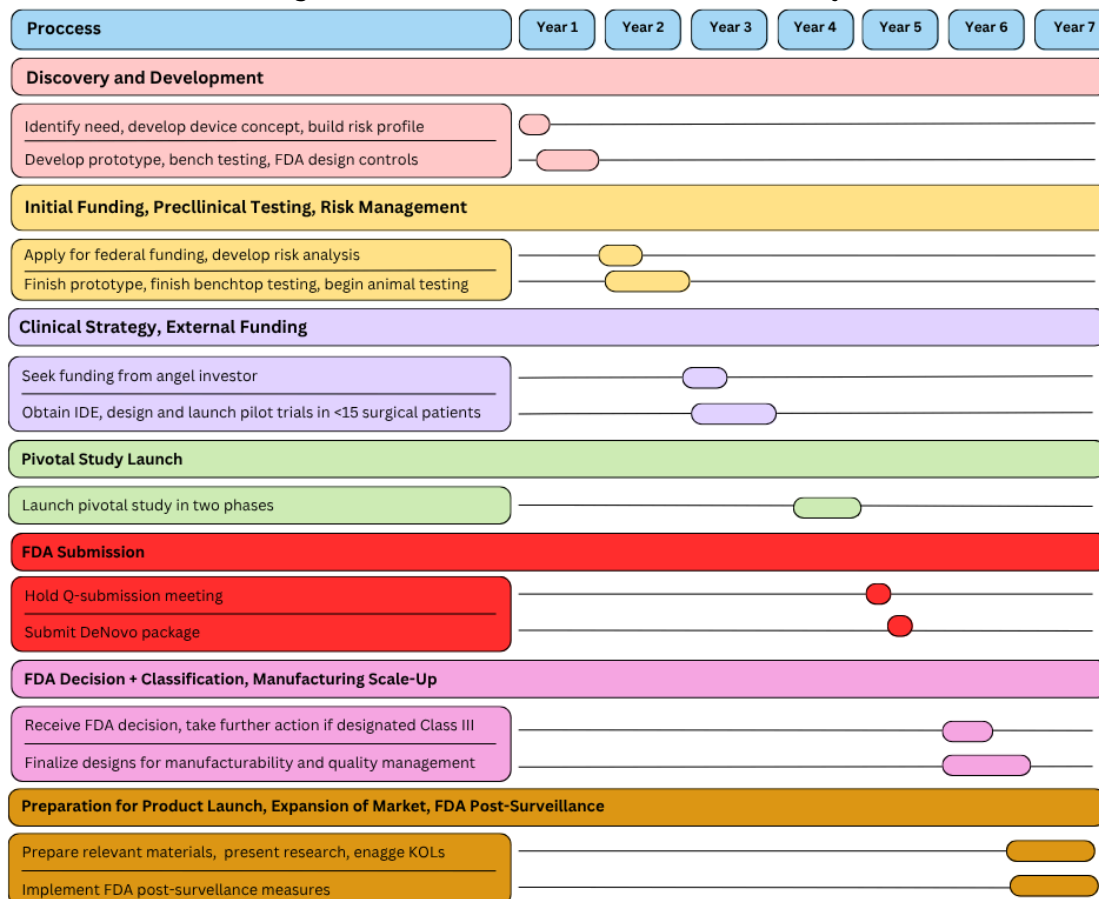
The average absorbance across all samples before CV was  $0.132 \pm 0.001$  and after CV was  $0.134 \pm 0.002$ . These values from the MOF samples were nearly identical to the water blank (0.128) and far below the copper standard (0.468), indicating no detectable copper was released into solution. Based on Table A1 below, this outcome supports what we expected and suggests that the MOF keeps its copper stably bound under these conditions. With Nafion<sup>TM</sup> providing an additional barrier, these results strongly support safe *in vivo* use of our biosensor.

**Table A2.** Colorimetric copper assay results.

MOF Sample #	1	2	3	4	Average	Standard Deviation
Absorbance Before CV	.133	.132	.133	.131	.132	.001
Absorbance After CV	.135	.133	.135	.132	.134	.002

## 8.9. Major Milestones

**Fig. A14.** 7-Year Gantt Chart to commercial availability.



### Year 1 Milestones

**Discovery & Planning:** Many of our Year 1 discovery and planning milestones were achieved through participation in the SensUs competition. Our clinical need - continuous creatinine monitoring in post-operative patients for early detection of PO-AKI - was identified through interviews with patients and healthcare professionals specializing in kidney health and post-surgical care. Key insights from these interviews are outlined in Section 4.1, including the patient burden of hospital stay after surgery and the significant number of annual PO-AKI cases globally. The decisive factor in targeting hospitals as our primary market was the costly alternative for PO-AKI monitoring during overnight patient observation.

Aligned with this clinical need and target population, we developed a medical device concept with clearly defined performance requirements. Using CAD modeling, we created prototypes and shared them with patients, physicians, and industry experts to refine our final design, illustrated in Fig.

A15. We also evaluated the financial feasibility of this design by comparing overnight

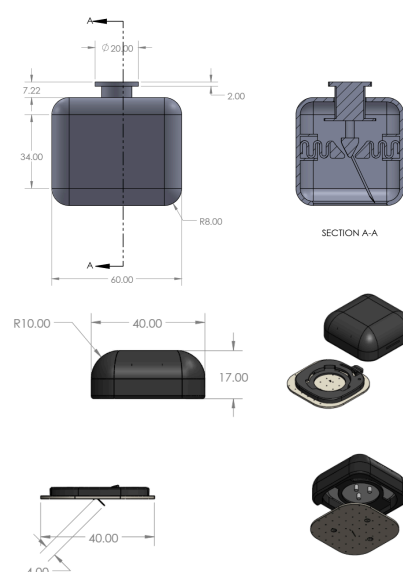


**Fig. A15 :** Computer Aided Design (CAD) drawings of the applicator (top) and the wearable sensor (bottom)

patient monitoring to the cost of using our sensor from the lens of a startup company, as seen in Section 8.11 in of the appendix.

With the design complete, we now turn to building a comprehensive risk profile, covering both physical sensor components and data privacy concerns associated with our software. To support this, we will maintain a Design History File (DHF), as required by the Food and Drug Administration's (FDA) quality system regulation to market medical devices in the US. The DHF will document the device's design, manufacturing processes, outsourced work, and any issues encountered, enabling traceability of risks to specific components or processes. This file also supports future regulatory approval in international markets, as it requires the gathering of information necessary for approval in these countries.

**Developing Prototype and Design Controls:** After the discovery and planning phase was completed, an alpha-prototype was developed for early bench testing, including a combination of CAD, printing, and bench models. Our initial prototype is presented through bench models for technical testing and a 3D-printed CAD model for observing the device's practicality through size and weight scalability. After developing early prototypes, we have conducted preliminary technical bench testing to ensure that our device is functional (can accurately detect varying levels of creatinine). This was done without a fully-functional sensor design, and solely tested the active sensing element of our future design.

Throughout the process of developing our alpha-prototype, it is crucial to apply FDA design controls (21 Code of Federal Regulations 820.30) to ensure our device is compliant with FDA stipulations (National Archives, 2025). These design controls encompass design/development planning, design input, design output, design review, design verification, design validation, design transfer, and design changes.

### **Year 2 Milestones**

**Initial Funding:** To allow for the device to continue being tested and developed, we plan to apply for government grants within the United States (US) to fund future benchtop and animal testing. First, we will apply through the National Institute of Health (NIH) due to their considerable annual budget (\$5.5 billion USD) for research funding. Specifically, we plan to apply to the Small Business Innovation Research (SBIR) and Small Business Technology Transfer (STTR) programs. These grants can vary from \$150,000 USD to \$1.5 million USD depending on the stage of development of the product (SeaCoast Financial, LLC, 2024). If these applications are unsuccessful, we plan to apply for SEED funding through America's Seed Fund - a department of the US National Science Foundation that grants funding to nearly 400 startups annually and encourages the transformation of engineering discoveries into products (Johnson, 2023).

**Preclinical Testing and Risk Management:** A more finalized product will be developed during the early months of Year 2 that expands off of successful benchtop testing with the alpha-prototype. This prototype will be a semi-finalized version of the final product that will be used to complete the remainder of benchtop testing. These tests are outlined in Section 4.2.3 and are used to validate the following components of the device: (1) Bluetooth™ connection of transmitter, (2) battery charge of potentiostat, (3) patch durability (4) usability/reusability of applicator, and (5) microneedle injection depth.

After benchtop testing is finalized, small and large animal testing will be conducted to ensure the safety of our sensor. These tests will be in accordance with the Animal Welfare Act, Animal Welfare Act Regulations, Public Health Service Policy of Humane Care and Use of Laboratory Animals and the Guide for the Care and Use of Laboratory Animals. All studies conducted will also be in accordance with the ISO 10993 series to manage risk with regards to biocompatibility. The tests conducted are outlined in Section 8.10.

The final milestone that will be achieved in Year 2 is the development of risk analysis per ISO Standard 14971. This standard documents specific terminology, principles, and a process for risk management of medical devices. The intention behind this standard is to develop a process to identify hazards associated with the medical device, estimate/evaluate associated risks, control these risks and monitor the effectiveness of the controls.

### **Year 3-4 Milestones**

**Clinical Strategy and Trials:** Following the successful completion of animal trials, the next key step in validating our device will be clinical trials. Before initiating these, we will obtain an Investigational Device Exemption (IDE) in the US, which permits the use of a development-stage device in a clinical study to gather safety and efficacy data. To ensure participant safety, our clinical trials will follow ISO Standard 14155 (Clinical Investigation of Medical Devices for Human Subjects - Good Clinical Practice) and ISO Standard 14971 (Application of Risk Management to Medical Devices). Good Clinical Practice (GCP), outlined in both of these ISO standards and Title 21 of the Code of Federal Regulations, includes requirements such as informed consent and Institutional Review Board approval (FDA, 2021).

Once the IDE is secured and the study designed, we will seek funding from an angel investor. As advised by Dr. Menegatti, our goal is to raise \$30-50 million in exchange for 50% equity in our company. Angel investors typically invest personal capital in high-risk, high-reward ventures and often have investment experience. When approaching investors, we will present the IDE, study design, projected expenses, risk assessments, and financial forecasts, among other documents, to maintain transparency with our investors.

With funding in place, we will launch a pilot study with <15 surgical participants, as outlined in Section 8.9. This initial phase will help identify improvements to study design, safety protocols, and overall efficacy. The procedure will be refined based on these findings before initiating a larger-scale pivotal study involving several hundred participants to confirm the pilot study's results.

### **Year 5 Milestones**

**Pre Submission (Q-Sub) Strategy, Submission Preparation:** Following the completion of safe and effective clinical trials, we plan to apply for a Q-submission meeting with the FDA to confirm eligibility for the DeNovo pathway and align data expectations. This application will consist of a cover letter, thorough description of a medical device, proposed use of the device, mechanism of action within the body, and technological characteristics. This will be done 2-6 months before DeNovo package submission (Emergo, n.d.).

After this meeting, we are planning to submit our DeNovo package to the FDA. This package will include the device description, intended use, technical specifications, proposed risk controls, manufacturing information, quality management systems evidence, and labeling requirements. All non-clinical and clinical data will also be included to ensure the safety and efficacy of our device. This package will be submitted alongside the \$145,000 USD user fee payment for the submission of a DeNovo request for a small business.

### **Year 6 Milestones**

**FDA Review, Decision, and Classification:** Year 6 will be the final year of development for the product and all regulatory controls. The FDA will check for the completeness of 21 Code of Federal Regulations 860.230 (accepting a DeNovo request) within a 15 calendar day period. This is classified as the acceptance review period and is a prerequisite for the substantive review period.

Once the acceptance review is completed, the FDA will move along with the substantiated review. This section of the approval process will evaluate eligibility, sufficient controls, clinical/non-clinical evidence and benefits vs. risks. If deficiencies are found, the FDA issues an additional information letter, which pauses the review clock. A completed response will be required within 180 days if an additional information letter is issued.

Once the acceptance and substantiated reviews are completed successfully, the FDA will issue a formal classification of the device as Class I or Class II with special controls. If these reviews are completed unsuccessfully, the device will be grouped as a Class III device until further action is taken (U.S. Food and Drug Administration, 2024).

**Manufacturing Scale-Up and QMS Validation:** During this entire review process, we plan to simultaneously finalize designs for manufacturability. Specifically, installation qualifications (IQ), operational qualifications (OQ) and performance qualifications (PQ) will be submitted as documented verification processes, along with documents detailing

packaging and sterilization processes (The FDA Group, 2024). A full quality management system (QMS) in accordance with ISO Standard 13485 and 21 Code of Federal Regulations 820 will be developed, suppliers will be audited and final QMS validation will take place.

### **Year 7 Milestones**

***Preparation of User Manuals, Training Materials, Marketing Assets:*** Year 7 will be the year our product will be available to commercial markets. User manuals, training materials, and marketing assets will be prepared to release with the sensor device. User manuals will be developed in accordance with 21 Code of Federal Regulations 801 and 21 Code of Federal Regulations to satisfy labeling requirements and design controls. Training materials will be developed and aligned with ISO Standard 20417:2021, ISO/TR 62366-2:2016, and ISO Standard 13485, which outlines the need for training records. Marketing assets will be created in accordance with 21 Code of Federal Regulations 801.6 and ISO 13486:2016 clause 7.3, ensuring advertising materials are not false or misleading.

***FDA Post-Surveillance:*** Once all relevant materials have been produced, we plan to implement surveillance controls to comply with the FDA throughout the production process. An important section of the Code of Federal Regulations (CFR) we will pay special attention to is 21 CFR Part 803 - this outlines mandatory reporting of any adverse events by manufacturers, importers, and users. Any safety issues regarding our device will be reported within 30 days to satisfy this section of the CFR. Another key regulatory control we will be following is Section 522 of the FDA Cosmetic Act - this stipulates that the FDA can require additional studies for Class II or III devices to collect data on performance after the product is launched. We expect to be conducting these studies throughout the post-market surveillance process considering our device would be classified as Class II. Additionally, we will plan to continuously collect real-world data from EHRs that are linked to our CreaCare software - this will allow us to identify negative trends early and adjust accordingly. Finally, any corrections or recalls will be conducted in accordance with 21 CFR part 806. By following these main post-surveillance regulatory controls, we plan to continuously monitor our product for safety and efficacy and adjust production accordingly.

***Publish Clinical Data, Present at Conferences, Engage Key Industry Leaders:*** After accompanying materials for our device have been developed and validated, we plan to publish clinical data gathered in Years 3-4, specifically from the pivotal studies. First, we plan to submit our data to the NIH's [ClinicalTrials.gov](https://clinicaltrials.gov) database where all studies are viewable to the public. The format of the data submitted will be revised and reevaluated based on peer-reviewer questions (National Library of Medicine, 2025). We then plan on submitting papers detailing the biosensor's specifications and clinical data regarding our biosensor's performance to the following journals: *Biosensors and Bioelectronics*, *Biosensors*, and *International Journal of Biosensors and Bioelectronics*. The content will be edited according to peer-reviews submitted.

During the publishing process, we will also present our data at conferences. We aim to present at the following conferences: Biosensors Conference, International Conference on Bio-Sensing Technology, and Bio-IT World Conference and Expo. These conferences were specifically chosen to help connect with key opinion leaders (KOLs) that can help expand our market internationally, specifically to EU countries following the US launch.

Following the 7-year launch of our product in the US, we plan on expanding our market to EU countries. The path to regulating this product within the European Union can be seen in Section 8.12 of the appendix.



## 8.10. Future Research Plan: Pre-Clinical & Clinical Trials

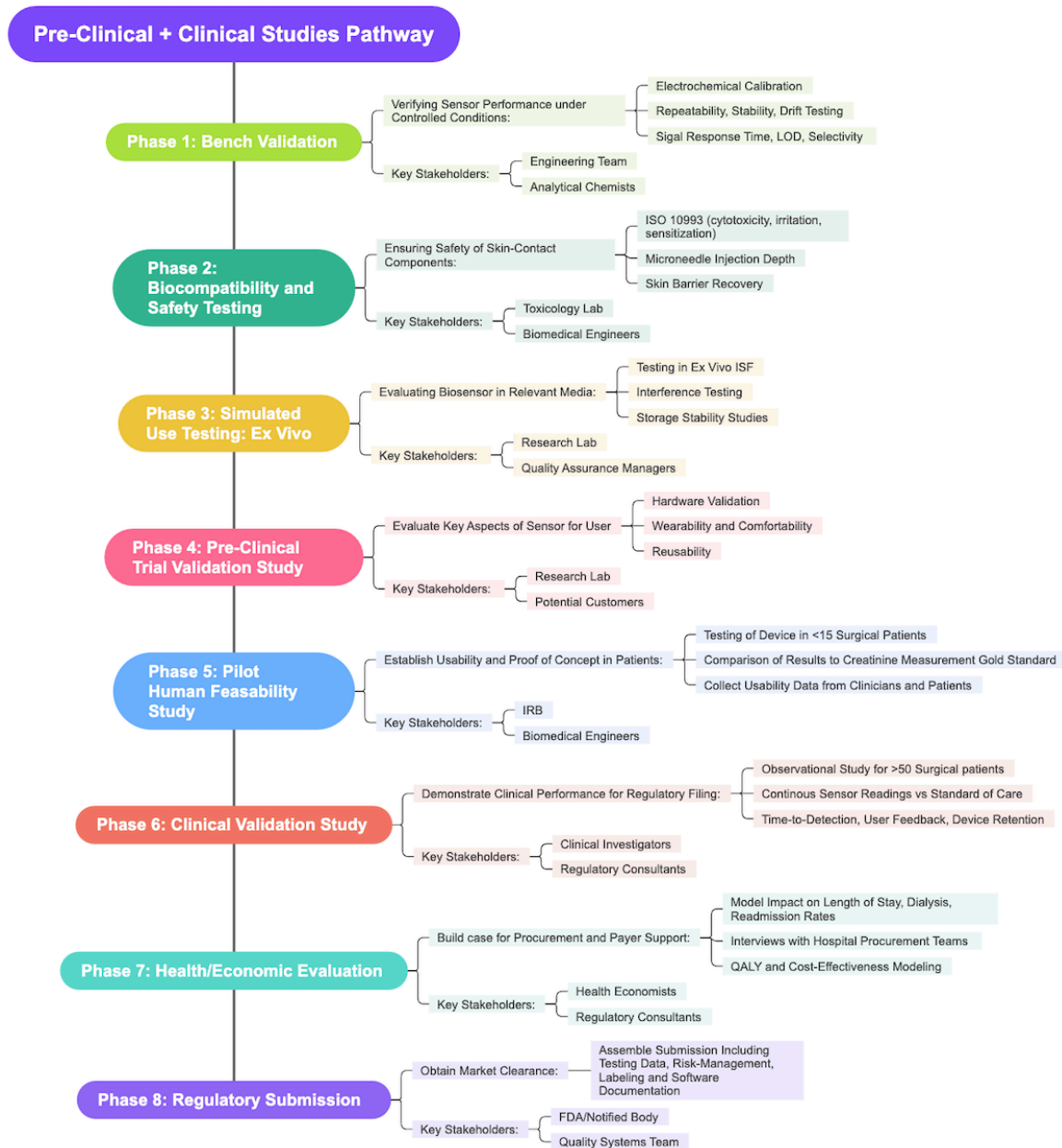


**Fig. A16.** Phases of Pre-Clinical and Clinical Trials

**Table. A3.** Phases of Pre-Clinical and Clinical Trials and Associated Deliverables

Phase	Goal	Key Activities	Stakeholders	Deliverables
1. Bench Validation	Verify sensor performance under controlled conditions	<ul style="list-style-type: none"> <li>- Electrochemical calibration in PBS and simulated ISF</li> <li>- Repeatability, stability and drift testing</li> <li>- Signal response time, LOD, selectivity testing</li> </ul>	<ul style="list-style-type: none"> <li>- Engineering teams</li> <li>- Analytical chemists</li> </ul>	<ol style="list-style-type: none"> <li>1. Sensor performance specification sheet</li> <li>2. Calibration curves</li> <li>3. Defined operating range</li> </ol>
2. Toxicity and Safety Testing	Ensure safety of components contacting skin	<ul style="list-style-type: none"> <li>- Cytotoxicity, irritation, sensitization testing (ISO 10993)</li> <li>- Assessment of microneedle injection depth and associated skin barrier recovery</li> </ul>	<ul style="list-style-type: none"> <li>- Toxicology lab</li> <li>- Biomedical engineers</li> </ul>	<ol style="list-style-type: none"> <li>1. Biocompatibility report</li> </ol>
3. Simulated Use Testing: <i>Ex Vivo</i>	Evaluating biosensor in relevant media	<ul style="list-style-type: none"> <li>- Testing in <i>ex vivo</i> ISF</li> <li>- Interference testing</li> <li>- Shelf life and storage testing</li> </ul>	<ul style="list-style-type: none"> <li>- Research lab</li> <li>- Quality assurance team</li> </ul>	<ol style="list-style-type: none"> <li>1. Functional stability data</li> <li>2. Data interference matrix</li> <li>3. Technical file inputs</li> </ol>
4. Pre-Clinical Trials Validation Study	Establish usability in healthy individuals	<ul style="list-style-type: none"> <li>- Assessment of device in healthy individuals</li> <li>- Wearability, durability, comfortability testing</li> </ul>	<ul style="list-style-type: none"> <li>- Research lab</li> <li>- Potential customers</li> </ul>	<ol style="list-style-type: none"> <li>1. Patient comfort data</li> <li>2. Wearability data</li> <li>3. Durability data</li> </ol>
5. Pilot Human Feasibility Study	Establish usability + proof of concept in patients	<ul style="list-style-type: none"> <li>- Deploy device in 15 post-op surgical patients</li> <li>- Compare biosensor readings with gold-standard creatinine measurements</li> <li>- Collect usability data from clinicians and patients</li> </ul>	<ul style="list-style-type: none"> <li>- IRB</li> <li>- Clinicians</li> <li>- Biomedical engineers</li> </ul>	<ol style="list-style-type: none"> <li>1. Feasibility and usability report</li> <li>2. Paired serum vs ISF creatinine correlation data</li> <li>3. Iterations for design optimization</li> </ol>
6. Clinical Validation Study	Demonstrate performance for regulatory filing	<ul style="list-style-type: none"> <li>- Deploy device in 50 post-op surgical patients</li> <li>- Compare biosensor readings with gold-standard creatinine measurements</li> <li>- Evaluate correlation, time-to-detection, user feedback</li> </ul>	<ul style="list-style-type: none"> <li>- Clinical investigators</li> <li>- Regulatory consultants</li> </ul>	<ol style="list-style-type: none"> <li>1. Clinical performance report</li> <li>2. Statistical analysis of sensitivity/specificity</li> <li>3. Human factors/usability engineering report</li> </ol>
7. Health and Economic Benefits	Build case for procurement and payer support	<ul style="list-style-type: none"> <li>- Model impact of device on LOS, dialysis, readmission rates</li> <li>- Conduct interviews with hospital procurement</li> <li>- Cost-effectiveness modeling</li> </ul>	<ul style="list-style-type: none"> <li>- Health economists</li> <li>- Hospital partners</li> </ul>	<ol style="list-style-type: none"> <li>1. Economic impact model</li> <li>2. Procurement value proposition</li> <li>3. Support for reimbursement discussions</li> </ol>
8. Regulatory Submission	Obtain market clearance	<ul style="list-style-type: none"> <li>- Assemble regulatory package</li> <li>- Include risk management, testing data, labeling, software documentation</li> </ul>	<ul style="list-style-type: none"> <li>- Regulatory team</li> <li>- Quality systems</li> <li>- Notified body</li> </ul>	<ol style="list-style-type: none"> <li>1. Regulatory submission package</li> <li>2. Post-market surveillance plan</li> </ol>

### 8.10.1. Small Animal Testing

Following the successful completion of benchtop testing (Section 4.2.3), pre-clinical studies will be conducted through a partnership with Pacific BioLabs. In compliance with ISO Standard 10993, medical device toxicity testing will be completed in four stages before proceeding to clinical trials.

In the first stage, cytotoxicity will be tested *in vitro* on mammalian cells through the Direct Contact method in compliance with ISO Standard 10993-5, ensuring our microneedle technology does not imply any directly toxic effects when submerged in subcutaneous tissue. In the second stage, device extractables and leachables will be tested in compliance with ISO Standard 10993-18 in order to obtain chemical characterization and analysis of the biosensor's components. This also secures a toxicological risk assessment of possibly harmful chemicals prior to biological and clinical

testing. In stage three, hemolysis testing will be conducted in accordance with American Society for Testing and Materials (ASTM) Standard F756 and ISO Standard 10993-4 via direct and extract methods to evaluate the adverse effects of our biosensor on rabbit blood. Despite the fact that our biosensor does not come into direct contact with human blood, this ensures that any leachables that do come into contact with blood do not cause adverse reactions. In the fourth and final stage, *in vivo* testing will be conducted in rat and mice models, including skin irritation testing and systemic toxicity testing. Once these results are optimized through Pacific BioLabs, we will proceed to custom large animal studies.

In order to validate the single use of microneedle/patch applications in a clinical environment, our microneedle/patch package will undergo ethylene oxide sterilization validation testing following various ISO standards through Pacific BioLabs. This will optimize sterilization cycle parameters and ensure cleanliness in both clinical trials and hospital use (Pacific BioLabs, 2025).

#### 8.10.2. Large Animal Testing

Once our device has successfully completed toxicity trials in small animals, large animal testing must be completed to further validate our device's safety. We plan on partnering with North American Science Associates (NAMSA), a key contract research organization that provides testing and regulatory services for medical device researchers. We plan on conducting all tests in swine as their anatomy most similarly mimics humans.

All trials conducted will be in accordance with ISO Standard 10993-1 Annex A and the 2023 FDA biocompatibility Guidance document. ISO Standard 10993-1 Annex A is a multi-part standard that outlines numerous tests that are used to confirm the safety of our device. The relevant tests conducted will be conducted in the order they are mentioned.

First, part 2 of ISO Standard 10993-1 Annex A outlines animal welfare requirements and requires justification of animal use, species and numbers used, required trained personnel, approved protocols by the Institutional Animal Care and Use Committee (IACUC), appropriate husbandry, humane endpoints, documentation of results following Good Laboratory Practices. Although not a scientific "test," this part of the relevant ISO standard is crucial for further tests to be conducted.

The next part of this relevant ISO standard that is to be evaluated is genotoxicity, carcinogenicity, and reproductive toxicity. This is intended to determine if any DNA mutations or chromosomal damage is observed. Two different tests must be conducted to detect the two major classes of genetic damage using mammalian cells, and we plan to use a chromosomal aberration assay (OECD) and mammalian cell micronucleus test (OECD 487) to evaluate this aspect of the device's toxicity.

Although not required for our device considering it does not make direct contact with blood, we plan on conducting tests with regards to hemocompatibility to ensure any leaching that occurs in our sensor will not cause adverse effects. We plan to conduct an *in-vivo* leukocyte count assay (ASTM Standard F2888-19) which is intended to evaluate the potential of leachables to affect platelets and leukocytes in mammalian cells.

The next step for conducting large animal testing in accordance with ISO Standard 10993-1 Annex A is to evaluate cytotoxicity *in-vitro* in mammalian cells. Both qualitative (morphology, vacuolization, lysis...) and quantitative (cell death, inhibition of cell growth, cell proliferation...) metrics will be used to evaluate the system's cyto-toxicity in a sample of cultured cells from our swine.

A key aspect of this relevant ISO standard that will be tested next are implantation effects. After our device is implanted in the most clinically-relevant location of the swine, testing will be conducted based off of intended clinical exposure time and will mimic the PO-AKI monitoring period of ten days. Comparisons of tissue response to a control population of pigs will be observed as well as evaluation of macroscopic and microscopic effects.

We next must observe the effect of any polymer degradation on our systems safety, specifically with regards to the polyimide that is used in our electrode fabrication. The test

will be designed to mimic clinical use as much as possible and changes will be evaluated using mass balance and molecular mass distribution techniques.

Sensitization tests will be performed next to determine the potential of our device to cause an allergic reaction. A murine local lymph-node assay (LLNA) will be used to quantify lymphocyte proliferation following topical exposure of test extracts.

One of the largest tests conducted during this study will be the evaluation of systemic toxicity, which is used to determine the potential of a device to cause systemic toxicity over a specific duration of time. The route of administration of our device will be chosen to be most clinically relevant and negative controls will be employed. Acute tests will be performed with a single application of our device to observe symptoms across the first 72 hours. Other test durations will be observed as well. To evaluate our system's toxicity, metrics of serial evaluations of body weight, clinical observation, clinical chemistry, gross pathology, and histopathology of organ systems will be used.

The next step of conducting animal trials in accordance with ISO Standard 10993-1 Annex A will be to observe chemical characterization. Our device will be subjected to tests to evaluate the amount, identity, and characteristics of extractables. A combination of the following tests will be used to evaluate chemical characterization: fourier transform infrared spectroscopy (FTIR), gas chromatography with mass spectrometry (GC-MS) for detection of semi-volatile organic compounds (SVOC) and determination of trace metals using inductively coupled plasma mass spectrometry (ICP-MS).

Finally, to finish large animal testing conducted in swine, *in-vivo* tests will be conducted to evaluate dermal irritation after exposure to our device. Both single exposure and repeated exposure strategies will be employed to assess our device over longer periods (Swanson, 2025).

#### 8.10.2. Pre-Clinical Trials Validation Study

Once animal trials have been completed successfully in accordance with all ISO standards, a clinical validation study can be conducted as the next step for verifying the key elements of our sensor for the user. It is important to note, these are not clinical trials, but a study designed to validate certain aspects of our device as effective. Once this study is complete, we will have enough data to begin pilot and pivotal studies. These trials will test the following aspects of our device: (1) toxicity of sensor, (2) Bluetooth™ connection of transmitter, (3) reusability of applicator, (4) microneedle injection depth, (5) battery charge of the potentiostat, (6) durability of patch, (7) wearability, and (8) mode of feedback for potentiostat application. All relevant ISO standards will be followed, with special attention being paid to ISO Standard 14155 (Clinical Investigation of Medical Devices for Human Subjects - Good Clinical Practice) and ISO Standard 14971 (Application of Risk Management to Medical Devices).

To begin this study, 50 participants with no contraindicated health conditions are gathered via a volunteer basis and will be compensated with funding from the previously mentioned angel investor. These volunteers will be asked to wear the prototype sensor for 10 days and provide feedback as mentioned below. Participants will apply the patch directly to their triceps region and rate the ease of application and comfort on a scale of 1-10. An average score of 8 will be required for both of these tests to be considered a "pass." The patch will be observed throughout this process and further tests will be conducted to verify its effectiveness.

After the patch is applied, the reusable applicator will be used to apply the microneedle/electrode setup on top of the patch to each participant. The applicator will be sterilized in accordance with ISO Standard 17664 (Processing of Healthcare Products) between each use as this standard outlines the process for sterilizing reusable medical devices. The applicator will be scored using the same method detailed in the benchtop and animal testing (using dye injection + ultrasound imaging to assess microneedle depth and ensure it's within the 500 um to 1 mm passing range with a standard deviation of <50 um).

As mentioned in the benchtop testing section of the validation study, the FDA mandates an audible, visual and touchable mode of feedback once the potentiostat is applied. The next step of these clinical trials is to ensure these modes of feedback are all

present. This will be evaluated on a pass/fail basis as participants will be asked if they feel the potentiostat being applied, if they heard the audible “click,” and if they can visually see the potentiostat snapping onto the setup. All three modes of feedback must be verified by the participant for the device to pass.

The microneedle/electrode setup's toxicity can be evaluated similarly to the methods outlined in the benchtop and animal testing. Participants will be asked to rate the level of inflammation/irritation where the device is applied each day on a scale of 1-10 (1 being no inflammation, 10 being unbearable inflammation).. An average score of 2 across all participants is required for the device to pass. Additionally, an enzyme-linked immunosorbent assay (ELISA) will be conducted prior to microneedle application and at the end of the 10 day trial to quantify the amounts of relevant cytokines (IL-1, IL-6, IFN, and TNF- $\alpha$ ). A doctor will be contracted during this portion of the study to verify that the increase in cytokines does not constitute a cytokine storm (dangerous and potentially life threatening immune response) (Fajgenbaum et al, 2020).

The next stage of these clinical trials can evaluate the device's effectiveness outside of a controlled environment. The participants will be asked to go about their daily routines during the 10 day testing period and during this time, wearability of the sensor, battery charge of potentiostat, durability of patch, and Bluetooth™ connection of transmitter can be observed.

To observe the wearability of the device, participants will be asked daily to rate how much the sensor interfered with their daily tasks on a scale of 1-10 (one being unnoticeable, 10 being extremely obstructive). An average score of 3 will be required for the device to pass this trial.

The durability of the patch can be quantified using a similar approach. Volunteers will be asked to rate how well the patch adhered to their skin each day on a scale of 1-10 (1 being completely ineffective, 10 being perfect). Additionally, participants will be asked daily to rate how well the sensor held up when faced with sweat or other forms of liquid on a scale of 1-10 (1 being completely ineffective, 10 being perfect). An average score of 7 will be required for the device to pass each of these tests.

Bluetooth™ connection of the transmitter will also be evaluated periodically across the 10 day study period. At the end of each day, the individuals conducting the study will observe the continuous monitoring chart which displays continuous creatinine readings in the associated CreaCare software. The Bluetooth™ connection of the sensor will be evaluated on a pass/fail basis, with a pass constituting no loss of connection across the 24 hour period being evaluated. Any loss of connection will result in a failing grade for the Bluetooth™ aspect of this device.

Finally, the last aspect of the device these clinical trials aims to address is the battery life of the potentiostat. This can be simply evaluated by ensuring the potentiostat is charged to 100% at the beginning of the trial, and recording the charge left on the device. If the device has >20% charge remaining after the 10 day study period, the device will pass this test, if not, it fails.

### 8.11. Biosensor Cost-Effectiveness Rationale

The costs for a startup company producing our sensor are shown in table A3. were gathered using expert opinions and online sources and are shown in Table A3. This table represents the costs of production for a first-year startup that makes no profit in year one of operations.

The personnel costs that came out to \$736,000 USD annually include both salaries and benefits for 8 full-time employees with doctorate degrees working in R&D. These individuals will be paid an average of \$80,000 USD yearly, with benefits costing an additional 15% of salaries (\$12,000 per person).

**Table A4.** Cost of Production Breakdown for Year 1 of Startup

Item	Cost (USD)
Personnel	\$736,000
Infrastructure	\$22,750
Storage	\$9,264
Materials	\$550,000
Legal Fees	\$150,000
Software Fees	\$1,073,000
Advertising	\$50,000
Error Costs	\$518,203
Total Cost	\$3,109,217
Cost per Sensor	\$622

The infrastructure costs presented encompass the square footage of the laboratory used to develop these products. It is estimated that 4 lab benches (27.5 ft<sup>2</sup> per bench) and 4 large pieces of equipment (5 ft<sup>2</sup> per piece) would be required per lab to produce our product. This comes out to approximately 130 ft<sup>2</sup> used in the laboratory; this number is then multiplied by a factor of 2.5 to account for extra space in the lab, which equates to 325 ft<sup>2</sup> per lab. Two labs will be required to produce our product, which comes out to 650 ft<sup>2</sup> of space rented for production monthly. At \$28 USD charged per ft<sup>2</sup> per month for lab access, a cost of \$18,200 per month for lab space can be derived. This number was then multiplied by a factor of 1.25 to account for any unseen variance in cost, which comes to \$22,750 USD monthly in rent.

The cost of storage was found by estimating the size of the packaging for one of our sensors. The design of our sensor is based off of a continuous glucose monitor (CGM), so the packaging size for our sensor is estimated using the size of the box for a Dexcom G7 sensor box. These boxes are approximately 8 cm x 6.5 cm x 6.5 cm, coming out to a volume of 0.000338 m<sup>3</sup>. After estimating the size of our packaging, we found a quote in Raleigh, North Carolina that comes out to \$386 USD monthly for a 3.05 m x 5.79 m x 2.45 m (43.27 m<sup>3</sup>) climate-controlled storage unit (Extraspace Storage, 2025). We estimate that we can fill a maximum of  $\frac{2}{3}$  of the unit to ensure accessibility, which allows for 28.85 m<sup>3</sup> of usable space. Ideally, all of the 5,000 sensors that are planned to be produced in Year 1 of the startup can fit in this storage unit, however, we plan to double the amount of storage purchased to account for storage of materials. This comes out to two storage units at \$386 USD a piece monthly, for a total of \$772 USD spent on storage per month. Multiplying this value by a factor of 12 gives the cost of storage for the first year of the company, which equals about \$9,264 USD.

The cost of materials was calculated by finding the costs of all the major components of our sensor. Chemical costs for the metal organic framework equalled about \$0.04 USD per sensor, potentiostat parts costs came to about \$37.14 USD per sensor, microneedle components cost about \$35.51 USD per sensor and finally, electrode components equalled about \$37.20 USD per sensor. In total, the cost of materials for one sensor produced equals about \$109.89 USD, which can be rounded to an even \$110 USD per sensor. For the 5,000 sensors we plan to produce in Year 1 of the startup, the total cost of materials for that year equals about \$550,000 USD.

Our legal fees were estimated by first determining the amount of patents needed to protect our product. The applicator, potentiostat, and microneedle components of our device are all assumed to be open-source licensing via expert opinion, so we're assuming we would only need to patent the sensor as a whole. Our startup plans to launch this product in the US, so we're not planning on filing a Patent Cooperation Treaty (PCT) to provide protection in other countries within the first year. From here, we've consulted an expert with industry experience that estimated the following legal costs: \$40,000 USD for patent filing, \$100,000 USD for patent prosecution, and \$10,000 USD for yearly protection. This comes out to a total of about \$150,000 USD for first-year legal fees.

One of the largest costs in producing our sensor is software. This component is essential as it serves as the interface for displaying continuous creatinine measurements. Using online sources, we estimated year-one software costs. Development is projected at \$110,000 USD, covering research, planning, design, development, testing, and deployment, based on average figures from our source. Infrastructure is estimated at \$200,000 USD, representing the low-end cost of on-premise software suitable for EHS integration. Labor costs are projected at \$276,000 USD, assuming three developers earning \$80,000 USD annually, plus 15% for benefits. For EHR system development, our source indicated ready-made solutions cost about \$400,000 USD for small practices, which aligns with our startup's profile. HIPAA compliance fees for small organizations are approximately \$12,000 USD. Lastly, annual security and data protection costs—including maintenance, encryption, and access control—are estimated at \$75,000 USD. Altogether, first-year software costs are projected at approximately \$1,073,000 USD (Zolotarev, 2025).

Finally, after calculating all other overhead costs we can fix the cost of advertising. We set marketing costs at \$50,000, which was based on expert opinion via our supervisor, Dr. Mengatti.



In total, all costs combined equate to about \$2,591,014 USD spent in the first year of our startup. We also plan on multiplying our overhead costs by a factor 1.2 to account for an estimated 10% error rate in the production of our sensor. This comes out to \$518,202.80 USD budgeted for production errors and a total overhead cost of \$3,109,216.80 USD spent in year 1. If we're planning on producing 5,000 sensors in Year 1, we can derive a cost of around \$622 USD per sensor for hospitals assuming the company makes no profit initially. We approached finding the production costs from a position that's primarily focused on providing benefits to patients and hospitals rather than profitability. Considering our market penetration strategy aims to target 0.9% of our potential market in the US, we can assume there would be room to expand our market, even just within the US. Additionally, our product represents an extremely cost-effective solution for hospitals, which can be represented by comparing the cost of our sensor (assuming no profit) to the average cost of a night in the general ward within the US, which equates to roughly \$3,000 USD per night.

### 8.12. European Union (EU) Product Expansion

The *In Vitro* Diagnostic Regulation (IVDR) is a comprehensive set of regulations that governs the production and distribution of medical devices used to examine specimens derived from the human body for purposes such as diagnosis, monitoring, or disease production (European Parliament and the Council of the European Union, 2017). We confirm that this is the correct regulatory pathway for our sensor, as it analyzes interstitial skin fluid to detect creatinine levels. To potentially expand this to the European market, it is necessary to first classify our device according to the IVDR rules and then follow the corresponding conformity assessment pathway and timeline.

#### **Phase 1: Device Classification**

According to Article 47 of Regulation (EU) 2017/46, all *in vitro* diagnostic medical devices must be classified in accordance with Annex VIII, which defines a risk-based classification system (Classes A through D). Similar to a Continuous Glucose Monitor intended for diagnostic use, our device would be under Class C, specifically under Rule 3(j): "Devices intended for monitoring levels of substances or biological components, where erroneous results could lead to a patient management decision with significant risk to the patient" (European Parliament and the Council of the European Union, 2017).

Along with this, the device would be intended for near-patient testing since this device would be implemented and calibrated through the doctors to monitor the patients creatinine levels after an invasive surgery to prevent PO-AKI.

Throughout this period identification of economic operators such as the manufacturer, EU authorized representative, and more are assigned this is in accordance with Articles 10 through 14.

#### **Phase 2: Conformity Assessment:**

The conformity assessment is the process of verifying whether the device meets the specific standards or requirements, this can consist of groups reviewing the device documentation, safety standards, labeling, and risk management procedures. For Class C devices, the involvement of a Notified Body is required. These are organizations appointed by the European Union to assess whether a device complies with IVDR requirements. The Notified Body will evaluate whether additional clinical data, corrective actions, or approvals are required.

Given that our device falls under Class C, the following conformity assessment route would be followed.

**2.1: Quality Management System:** This system ensures compliance with regulatory, safety and performance requirements throughout the lifecycle of the IVD device. In accordance with Annex IX this system covers the design, manufacturing, clinical performance evaluation, vigilance, corrective and preventive actions, and post-market surveillance.

**2.2 Technical Documentation Assessment:** Throughout this process the designated Notified Body reviews the entire set of documentation to verify that the IVD device meets the safety and regulatory requirements of the IVDR. This assessment should not be done

through sampling since it is a Near Patient Testing (NPT) device which should only require thorough investigation of the technical documentation, this is in accordance with Annex II. Along with this, Annex III is dedicated to post market surveillance where we will produce the periodic safety update report which is required for Class C devices after the device has been on the market for a certain period of time. Additionally, the Summary of Safety and Performance is required which will be reviewed by the designated Notified Body.

### **Phase 3: Obtaining a UDI and registering our Medical Device in the European Database on Medical Devices**

To ensure traceability of the device, a Unique Device Identification (UDI) is obtained through a sequence of numerical characters that are created based on recognition and coding standards that serves as the access key which is used in databases. This number is also included in the packaging of our device to ensure authenticity. This information will then be reviewed by the manufacturer and will be uploaded to the European Database on Medical Devices (EUDAMED) and will be open to the public, this in accordance with article 28-29.

### **Phase 4: Notified Body Final Review & EU Declaration of Conformity**

Here the designated notified body will review the Quality Management System along with the full technical documentation. Along with this we will draw up the EU Declaration of Conformity which certifies that we comply and take full responsibility of the products compliance with the European law.

With all requirements completed, our device could be legally eligible for placement on the EU market. However, it is important to note that compliance with this regulation may differ for companies based outside the EU, such as American manufacturers seeking market access in Europe. The IVDR represents a significant shift from the previous *In Vitro* Diagnostic Directive (IVDD) and has only been fully in effect since May 2022. As a team, we are committed to staying informed and compliant with any updates or future regulatory changes that may impact the approval process for our device.

### **8.13. Stakeholder Interview Details**

**Mrs. Bress**, kidney transplant patient, provided valuable firsthand insights, sharing her experiences and concerns about kidney monitoring. Her input helped shape the understanding of patient needs and informed the design priorities for the biosensor.

**Mrs. Gilchrist**, a kidney disease patient, provided valuable patient perspective through her lived experience. Her insights helped inform the understanding of patient challenges, treatment adherence, and the impact of ongoing monitoring on quality of life.

**Mr. Wright**, a patent lawyer, helped us understand the patenting process and the importance of timing and strategy when protecting new inventions. His guidance gave us valuable insight into how to approach intellectual property as we develop our technology.

**Dr. Henderson**, VP of Product Quality Management at Kenvue, helped us to understand how quality management and supply chain strategies are critical in developing medical devices that meet regulatory standards. His insights from the healthcare industry (Johnson & Johnson) guided us in designing a scalable and manufacturable product ready for the medical market.

**Mr. Aaron**, Senior Director, Product Development at EyeCool Therapeutics, helped us understand the complex regulatory and manufacturing challenges for bloodstream devices, including biocompatibility testing, sterilization methods, and the potential 510(k) pathway using predicate devices like continuous glucose monitors. His insights on clinical benefits, cost-effectiveness, and early patent filing guided us to focus on proving the device's feasibility before scaling production.

**Dr. Wiggin**, CEO of Inoculus Ventures - Associate Professor at UNC-NC State Joint Dept. of Biomedical Engineering, clarified that our device will likely follow the DeNovo FDA

pathway due to its novel continuous monitoring function and contact with interstitial fluid, requiring thorough biocompatibility and sterilization testing. He emphasized tailoring our design and pitch to both scientific and business audiences, while focusing on user needs and preparing for regulatory and reimbursement challenges in both the US and EU markets.

**Dr. Probst**, a postdoctoral researcher from the University of North Carolina, guided us on navigating the De Novo pathway for our continuous sensor, emphasizing the importance of clinical validation and IP protection before targeting doctors and researchers. He also highlighted key technical challenges like copper biocompatibility and interference testing that we need to address for successful development.

**Mrs. McCoy**, Pediatric Renal Transplant Nurse Coordinator at The University of North Carolina, emphasized the critical need for continuous creatinine monitoring in pediatric kidney transplant patients to detect early signs of rejection and improve outcomes. She highlighted the importance of device accuracy, ease of use, and integration with hospital systems to support clinicians and families throughout the transplant care process.

**Dr. Vavalle**, Associate Professor of Medicine and Director, Training Program at The University of North Carolina in Cardiovascular Disease, highlighted that acute kidney injury (AKI) after major surgeries like open-heart procedures significantly increases patient risk and hospital stays, with creatinine trends being critical for monitoring recovery. He emphasized that continuous creatinine monitoring could help clinicians better assess kidney health post-discharge, improving patient outcomes and medication management.

**Dr. Sanderson**, Associate Professor of Medicine and Pediatrics and Director of Pediatric Dialysis, emphasized that creatinine monitoring after kidney transplant is essential and currently relies on frequent blood draws that can be burdensome for patients, especially those traveling long distances. He highlighted that a continuous, home-based creatinine sensor could greatly improve patient quality of life by reducing hospital visits and enabling more effective telehealth management.

**Dr. Parker**, a second-year Adult Nephrology Fellow at UNC, emphasized that post-transplant creatinine monitoring typically occurs daily in-hospital and weekly after discharge, with trends being more clinically valuable than isolated readings. She highlighted that transportation barriers can prevent rural and elderly patients from getting regular lab work, making a remote monitoring solution especially impactful.

**Dr. Jain**, Associate Professor of Medicine and Director, Nephrology and Hypertension Training Program, highlighted key considerations for app design, recommending flexibility in data display, such as toggling between eGFR and creatinine, and emphasizing that physicians should review trend graphs before sharing with patients to avoid anxiety. She noted that post-operative AKI is relatively common and influenced by factors like age and baseline kidney function, with treatment tailored to the underlying cause.

**Dr. Kotzen**, MD specializing in Nephrology and Transplant care, across both adult and pediatric populations at the University of North Carolina, emphasized the lengthy four to eight year wait time for deceased donor kidneys and the importance of early CKD detection and planning. She noted that post-transplant creatinine monitoring is intensive initially, daily while inpatient and tapering to monthly by four to six months, and that patients' understanding typically centers on trends in creatinine rather than eGFR values.

**Dr. Hubbard**, a teaching associate professor and commercialization strategist at The University of North Carolina, helped us develop a regulatory and commercialization plan, ensuring we meet biocompatibility and quality standards. He also supported us in defining the clinical need, preparing patent filings, and building a business strategy to position our device effectively in the market.

**Dr. Gbadegesin**, Associate Dean for Physician-Scientist Development at the Office of Physician-Scientist Development (OPSD) in the Duke University School of Medicine. He helped our team by providing critical insights into pediatric kidney transplant care, including detailed monitoring practices for creatinine levels post-surgery and patient education on kidney function metrics. His expertise guided us on clinical workflows, patient needs, and key device features such as accuracy, safety, and hospital integration essential for pediatric nephrology settings.

**Dr. Alqurini**, a Nephrologist from the University of Arkansas for Medical Sciences (UAMS), recommended a wearable microneedle device with an app for early monitoring of kidney transplant and advanced kidney disease patients to potentially reduce clinical visits and hospitalizations. She emphasized the importance of accuracy, patient usability, and the need for clinical trials and cost-benefit analysis to support hospital adoption.

**Dr. Marston**, MD, Professor and Associate Chair of Clinical Trials from the University of North Carolina, highlighted that hospital stays after surgeries like aneurysm repair typically last two to seven days, with AKI frequently extending these stays. He emphasized that continuous creatinine monitoring could enable earlier detection and treatment of AKI, supporting earlier discharge and effective at-home patient management.